Living on the edge of stability, the limits of the nuclear landscape

C. Forssén

Department of Fundamental Physics, Chalmers University of Technology, SE-412 96 Göteborg, Sweden

G. Hagen

Physics Division, Oak Ridge National Laboratory, Oak Ridge, TN 37831, USA
Department of Physics and Astronomy, University of Tennessee, Knoxville, TN 37996, USA

M. Hjorth-Jensen

National Superconducting Cyclotron Laboratory and Department of Physics and Astronomy, Michigan State University, East Lansing, MI 48824, USA
Department of Physics and Center of Mathematics for Applications, University of Oslo, N-0316 Oslo, Norway

W. Nazarewicz

Department of Physics and Astronomy, University of Tennessee, Knoxville, TN 37996, USA
Physics Division, Oak Ridge National Laboratory, Oak Ridge, TN 37831, USA
Institute of Theoretical Physics, Warsaw University, PL-00681 Warsaw, Poland

J. Rotureau

Department of Fundamental Physics, Chalmers University of Technology, SE-412 96 Göteborg, Sweden

Abstract. A first-principles description of nuclear systems along the drip lines presents a substantial theoretical and computational challenge. In this paper, we discuss the nuclear theory roadmap, some of the key theoretical approaches, and present selected results with a focus on long isotopic chains. An important conclusion, which consistently emerges from these theoretical analyses, is that three-nucleon forces are crucial for both global nuclear properties and detailed nuclear structure, and that many-body correlations due to the coupling to the particle continuum are essential as one approaches particle drip lines. In the quest for a comprehensive nuclear theory, high performance computing plays a key role.

1. Introduction

To understand why nucleonic matter is stable is one of the overarching aims and intellectual challenges of basic research in nuclear physics. To relate the existence and properties of nuclei to the underlying fundamental forces and degrees of freedom, is central to present and planned rare isotope facilities, see for example Refs. [1–8]. Important properties of nuclear systems are binding energies, radii, density distributions of nucleons, spectra, and decays. These quantities convey important information on the individual-nucleon motion manifesting itself in the shell structure of nuclei, including the appearance and disappearance of magic numbers, interplay between high-j unique-parity orbits and natural-parity states, and the rapid changes of nuclear properties around the reaction thresholds.

To relate the stability of nucleonic matter at various energies and length scales† to the underlying fundamental forces is a major quest for theoretical modeling. A multiscale approach is required which incorporates different degrees of freedom at relevant length and energy scales. Unfortunately, quantum chromodynamics (QCD), the underlying theory of the strong interaction, is highly non-perturbative in the energy region characteristic of nuclear structure. This region is governed by nucleonic (and sometimes mesonic) degrees of freedom. This requires an effective theory, usually framed as chiral effective field theory (EFT), which is consistent with the symmetries of low-energy QCD and the separation of scales relevant to the low-energy nuclear many-body problem. Linking different scales is far from easy. A key challenge is to understand the link between QCD and effective field theories. Interactions derived from these low-energy theories carry also a dependence on an energy scale, defined in terms of an energy cutoff Λ, that separates the Hilbert space of interest from its higher-energy complement. The cutoff is usually chosen so that it is possible to reproduce nucleon-nucleon (NN) scattering phase shifts up to ~ 300 MeV laboratory kinetic energy, which requires $\Lambda \sim 500 - 700$ MeV. For details, we refer the reader to the recent reviews [9, 10].

An important question is to understand the role of many-nucleon forces from chiral EFT in the nuclear medium. Furthermore, using EFT-based interactions in a many-body environment entails the development of proper many-body theories that allow for first principle calculations. There are other issues as well, such as the estimation of theoretical errors. For example, most many-body methods applied to the nuclear many-body problem involve basis set expansions. The errors which arise due to basis truncations need proper quantifications and clarifications [11–14]. Finally, a proper link between first-principle methods (which are of limited use when very many degrees of freedom are at play) and approaches based on the density functional theory, is essential if one wishes to understand nuclei and nuclear matter from a bottom-up perspective [15, 16].

† A simultaneous description of nuclei and neutrons stars in terms of hadronic degrees of freedom constitutes a daunting theoretical challenge as the length scale spans over 19 orders of magnitude, from several 10^{-15} m (nuclear radii) to approximately 12 kilometers (neutron star radii).

Neutron-rich nuclei are particularly interesting for this endeavor. As the neutron number increases within a particular chain of isotopes, one eventually reaches the limit of stability, the neutron drip line, where isotopes with additional neutrons are not neutron-bound anymore. The appearance or absence of magic numbers, formation of neutron skins and halos, and detailed tests of shell structure at the limit of neutron-to-proton asymmetry can be probed via investigations of masses, radii, and excited states of neutron-rich nuclei. Examples of recent progress in the radioactive nuclear beam (RNB) science are measurements of masses with Penning traps coupled to radioactive beams and nuclear charge radii and moments using laser spectroscopy techniques. New experimental data in the neutron-rich territory are crucial for constraining theoretical models of nuclei and astrophysical processes, see, e.g., Refs. [17, 18]. To put things in perspective, Fig. 1 shows the expected experimental information on the Ca isotopic chain that will be obtained at the future Facility for Rare Isotope Beams (FRIB).
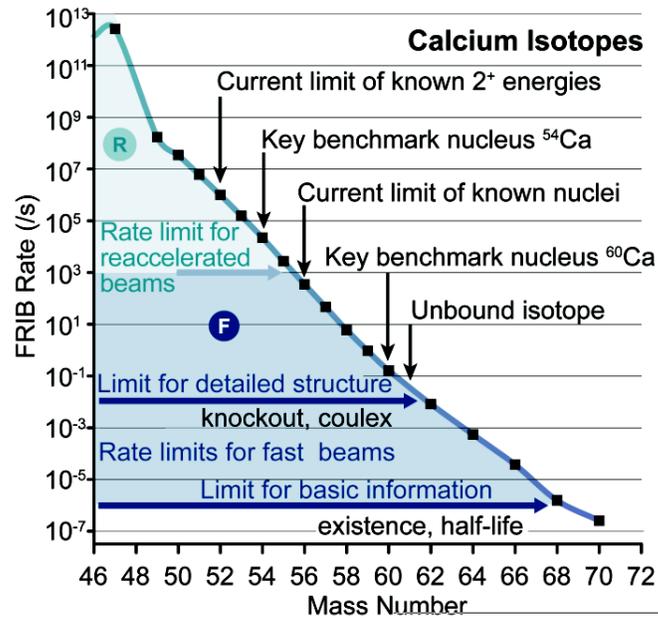

Figure 1. Expected experimental information on the calcium isotopes that can be obtained at FRIB. The limits for detailed spectroscopic information are around $A \sim 60$. (Courtesy of Brad Sherill [19].)

Having access to precise measurements of masses, radii, and electromagnetic moments for a wide range of nuclei allows to study trends with varying neutron excess. A quantitative description of various experimental data with quantified uncertainty still remains a major challenge for nuclear structure theory. Global theoretical studies of isotopic chains, such as the Ca chain in Fig. 1, make it possible to test systematic properties of effective nuclear interactions. Such calculations also provide critical tests of limitations of many-body methods. As one approaches the particle emission thresholds, it becomes increasingly important to describe correctly the coupling to the continuum of decays and scattering channels [20, 21]. While the full treatment of antisymmetrization

and short-range correlations has become routine in *ab initio* approaches to nuclear bound states, the many-body problem becomes more difficult when long-range correlations and continuum effects are considered.

This paper is organized as follows. Section 2 outlines modern theoretical approaches to the nuclear many-body problem, starting with renormalization schemes for nuclear forces and ending with a discussion of various many-body methods, in particular aimed at describing systems near the nucleon drip lines. Section 3 presents selected results for stable and weakly bound systems, with an emphasis on long isotopic chains. Conclusions and suggestions for future work are contained in Sec. 4.

2. Theoretical foundations

The task of developing a comprehensive theoretical framework that would be quantitative (i.e., capable of reproducing and explaining existing experimental data), have predictive power (i.e., capable of massive extrapolations), and provide uncertainty quantification (i.e., theoretical error bars) is daunting. To this end, theoretical models must meet three stringent requirements: (i) input (interactions, functionals) must be of high quality; (ii) many-body dynamics and correlations must be accounted for; and (iii) the associated formalism must take care of open-quantum-system aspects of the nucleus.

Solving the nuclear many-body problem is a challenging endeavor, since "exact" solutions exists only for the very lightest systems and closed form solutions only for highly-idealized, non-realistic cases. Over the last few decades there has been tremendous progress in developing many-body *ab initio* techniques capable of treating light and medium-mass systems. The state-of-the-art methods are based on controlled approximations and the underlying computational schemes account for successive many-body corrections in a systematic way.

The currently used theoretical techniques include: coupled-cluster methods [22–24], Quantum Monte Carlo applications [25–27], perturbative expansions [28], Green's function methods [29, 30], correlation operator methods [31], the density-matrix renormalization group [32–34], density functional theory [8, 35], in-medium similarity renormalization group [36, 37], and large-scale diagonalization methods [38, 39].

In low-energy nuclear physics, baryons (protons, neutrons, and possibly deltas), and mesons (pions and possibly other mesons with masses below 1 GeV) are considered to be the appropriate degrees of freedom, meaning that one can derive effective Hamiltonians based on the interactions between these constituents. Those Hamiltonians are derived from Lagrangians that are consistent with the symmetries of low-energy QCD using chiral perturbation theory at different orders (ν), in terms of a perturbative expansion using a hard scale Λ and a soft scale Q [10]. Within this picture, three-nucleon forces (3NFs) arise naturally since the interactions are derived for effective degrees of freedom at low energy, and heavier baryons and mesons are integrated out.

Currently, there are at least three different many-body methods for nuclear

structure with the capability to include both nucleon-nucleon interactions and 3NFs, yielding results that meet the few-body benchmarks. For light nuclei (with mass numbers $A \sim 12$), the Green's function Monte Carlo [40–42] and large-basis no-core shell-model (NCSM) approaches [39, 43, 44] have been successfully applied. These methods provide excellent results for two- and three-body Hamiltonians applied to light nuclei. However, for medium-mass and heavier nuclei, the dimensionality of the many-particle problem becomes intractable for these techniques. More recently, the coupled-cluster method has been applied to the structure of light and medium-heavy nuclei [24,45–47], providing excellent benchmarks for few-body systems such as ^{4}He [24]. This technique is best suited for treating nuclei around closed-shells but has very advantageous scaling properties that enable accurate calculations in very large model spaces. At the singles and doubles level of the method (expanding Slater determinants in terms of the exponential of one-particle-one-hole and two-particle-two-hole correlations), the number of floating-point operation scales as $n_o^2 n_u^4$, where n_0 and n_u are the numbers of hole and particle orbitals, respectively. Such soft scaling, when compared to the nearly combinatorial scaling of methods based on Hamiltonian diagonalization (as a function of basis size and/or particle number), allows one to build an extension of *ab initio* descriptions of nuclei all the way to medium and heavy systems.

Nuclear *ab initio* methods are now evolving to tackle a crucial challenge; the description of open nuclear systems. This development is timely since the overarching scientific questions of modern nuclear structure are about very neutron-rich or proton-rich nuclei whose properties are impacted by a coupling to the particle continuum of scattering and decaying states. Many nuclei of interest lie every close to particle emission thresholds, i.e., they are either short-lived or unstable. Such nuclei cannot be described in a closed quantum formulation, which assumes that the nucleons are artificially confined in a trap; hence, they are unable to decay.

It is therefore crucial for the nuclear many-body problem that new theoretical methods are developed that allow for an accurate description of loosely bound and unbound nuclear states. The recently developed complex-energy Gamow Shell Model (GSM) [48] has proven to be a reliable tool in the description of nuclei, where continuum effects cannot be neglected. In the GSM, a many-body basis is constructed from a single-particle Berggren ensemble [49–51], which treats bound, resonant, and scattering states on equal footing. Recently, GSM calculations of loosely bound and unbound states in nuclei, starting from a realistic interaction and a Gamow-Hartree-Fock basis were reported [52]. However, an *ab initio* description of light, unstable nuclei within the GSM approach will require novel many-body truncation schemes. In Ref. [53] the Berggren basis was employed for the first time in coupled-cluster calculations of the helium isotopes, and there are promising attempts to include the Berggren basis in an NCSM-like framework [54].

Finally, for the heavy and complex nuclei, the tool of choice is the nuclear Density Functional Theory (DFT) [55] and its extensions. Modern nuclear DFT is based on the mean-field approach rooted in the self-consistent Hartree-Fock-Bogoliubov (HFB)

problem. The DFT work is closely tied to *ab initio* studies of experimentally inaccessible systems such as neutron drops to enhance the predictive capabilities [56–58]. Important areas of research are the structure and decays of very neutron-rich nuclei, the dynamics of the fission process in heavy nuclei, and the structure of neutron star crust.

The quasiparticle HFB energy spectrum contains discrete bound states, resonances, and nonresonant continuum states [59–61]. That is, the effect of the particle continuum is naturally incorporated into the formalism, provided that the system of interest is particle-bound. In order to treat weakly-bound nuclei accurately, special care should be paid to the spatial extension of HFB states [61]. In this context, of particular interest are coordinate-space HFB approaches in large boxes [62], and PTG-HFB [63] and Gamow-HFB [64] frameworks.

The effective interaction in DFT, represented by the energy density functional (EDF), is characterized by a set of coupling constants constrained by experimental data and pseudo-observables determined by *ab initio* calculations. The uncertainty margins on EDF parameters are obtained by means of statistical methods like linear-regression with error analysis, which allows us to determine the correlations among EDF parameters, parameter uncertainties, and the errors of calculated observables [58,65–68]. Such an approach is essential for providing predictive capability and extrapolability, and for estimating the theoretical uncertainties. A representative example of DFT calculations containing uncertainty quantification, highly relevant to this paper, are the large-scale DFT calculations of Ref. [8] assessing the limits of the nuclear landscape. Quantifying the limits of nuclear binding is important not only for understanding the mechanism of nuclear binding, but also for understanding the origin of elements in the universe. Indeed, the astrophysical processes responsible for the generation of many heavy elements operate very closely to the drip lines; hence, the structure of very exotic, weakly bound nuclei directly impacts the way the elements are produced in stars.

In the following, we shall first briefly discuss models for the nuclear interactions and how these can be renormalized for truncated Hilbert spaces. Thereafter follows a brief description of configuration-interaction and coupled-cluster approaches to the nuclear many-body problem. We then discuss some developments that allow the study of open quantum systems within *ab initio* frameworks.

2.1. Realistic nuclear interactions

Ideally, the nuclear interactions should be derived from QCD, the underlying theory for the strong interaction. Unfortunately, the $^1S_0$ NN scattering length, a fundamental quantity characterizing the NN interaction, still remains a huge challenge for lattice QCD (LQCD) calculations, as the physical point (at the actual pion mass of 140 MeV) lies in a resonance in the unitary region [69]. In order to improve calculations, one needs to go to smaller lattice spacings, around $b = 0.05$ fm, but such computations require lattices of the order of $96^3 \times 193$ (the simulation cost grows as b^{-6}). Meanwhile, the LQCD computations for NN systems [70–73] provide important insights about the

basic properties of the nuclear force.

Several models of the NN interaction have been developed during recent years. These interactions reproduce NN scattering data up to 300-350 MeV laboratory energy with excellent precision [74–76]. The number of free parameters used in the fitting procedure is around 40. Being optimized to on-shell scattering data, various interaction models introduce different off-shell behavior resulting in different predictions for finite nuclei. (For more discussion on off-shell effects, see, e.g., Ref. [77].) The interaction models of Refs. [74–76] are either based on one-boson exchange with selected low-mass mesons, or are simply expressed in terms of local operators and optimized to data. More recently, due to a progress made in chiral-EFT [78, 79], several groups have constructed interaction models based on the underlying symmetries of QCD.

The starting point of the chiral-EFT is an approximation to the QCD Lagrangian. The chiral effective Lagrangian is given by an infinite series of terms with an increasing number of derivatives and/or nucleon fields, with each term being dependent on the pion field according to the rules of the broken chiral symmetry. Applying this Lagrangian to the NN scattering results in a systematic series of Feynman diagrams in a small parameter, the ratio of Q/Λ_χ, where Q is pion mass and $\Lambda_\chi \approx 1$ GeV is the chiral symmetry breaking scale. For a given order ν, the number of contributing terms is finite and calculable; these terms are uniquely defined, and the prediction at each order is model independent. By going to higher orders, the amplitude can be calculated to any desired accuracy. This scheme has become known as chiral perturbation theory (χPT).

Interactions derived from EFT have a number of advantages over traditional potential models. First, the corresponding currents are consistently formulated, and this is important for the correct description of observables other than the energy. Second, a power counting in terms of Q/Λ_χ exists for systematic improvements of the interaction and observables. Third, the hierarchy of NN forces, 3NFs, and higher-rank forces is explained by power counting. Three-nucleon forces enter at next-to-next-to-leading order (N²LO) order, and four-nucleon forces appear at N³LO. Recent work [10, 80] provides, for the first time, a chiral interaction of quantitative accuracy. The authors of Ref. [81] undertook the task of generating an accurate NN interaction based on chiral perturbation theory at N³LO order. The number of free parameters used in this chiral interaction is 24, which is similar to the number of free parameters used to parametrize other NN forces. Three-nucleon forces have been explored recently in light nuclei and neutron and nuclear matter [82, 83]. In light nuclei, chiral 3NFs affect the binding energy, radii and transition probabilities [39]. They are responsible for the anomalous long half life of ^{14}C [84]. In oxygen isotopes, they are believed to determine the position of the neutron drip line and the structure of neutron-rich isotopes [45, 85]. In calcium isotopes, 3NFs are important for our understanding of shell evolution and (sub)shell closures [86, 87]. Three-nucleon forces also affect properties of neutron matter [88–90] and the saturation of nuclear matter [83].

2.2. Derivation of effective interactions for truncated Hilbert spaces

The nucleon-nucleon interaction is strongly repulsive at short distances, meaning that a calculation which starts with the free interaction may converge very slowly. To overcome this problem, one defines effective interactions which can be used as starting points for calculations with basis-expansion approaches, such as the NCSM. The aim of this section is, therefore, to present and partly justify the computation of effective two-body Hamiltonians acting within a reduced Hilbert space.

The starting point is a translationally invariant two- or three-body realistic interaction. The first method discussed is based on a diagonalization of the two- or three-body Schrödinger equation in a large harmonic oscillator (HO) basis. In the two-body case, this basis typically consists of several hundreds of HO shells. Via a similarity transformation, one obtains an effective two-body interaction, acting within a reduced model space used in NCSM. Alternatively, one can diagonalize the Schrödinger equation in a full momentum space and then carry out a similarity transformation to a smaller space defined by some momentum cutoff Λ. This leads to the so-called low-momentum approach, or $V_{\text{low}-\text{k}}$, discussed below. We discuss also the so-called similarity renormalization group transformations.

2.2.1. Similarity transformed effective interactions in an oscillator basis
The translationally invariant Hamiltonian for an A-nucleon system, used in NCSM studies, is

$$H = \left[\sum_{i=1}^{A} \frac{\mathbf{p}_i^2}{2m} - \frac{\mathbf{P}^2}{2mA} \right] + \sum_{i<j}^{A} V_{NN}^{ij} + \sum_{i<j<k}^{A} V_{NNN}^{ijk}, \tag{1}$$

V_{NNN}^{ijk} is the three-nucleon force, and $\mathbf{P} = \sum_{i=1}^{A} \mathbf{p}_i$ is the center-of-mass momentum. Since we want to employ a HO single-particle basis, it is convenient to use the relation

$$\sum_{i=1}^{A} \frac{1}{2} m\Omega^2 \mathbf{r}_i^2 - \frac{m\Omega^2}{2A} \left[A^2 \mathbf{R}^2 + \sum_{i<j} (\mathbf{r}_i - \mathbf{r}_j)^2 \right] = 0, \tag{2}$$

where $\mathbf{R} = 1/A \sum_{i=1}^{A} \mathbf{r}_i$ is the center-of-mass coordinate and Ω is the oscillator frequency. Inserting this relation, we can rewrite the above Hamiltonian as $H(\Omega) = H_0 + H_I - H_{\text{CM}}$, where H_0 is the HO Hamiltonian, H_I is the interaction term defined by

$$H_I = \sum_{i<j}^{A} \left[V_{ij} - \frac{m\Omega^2}{2A} (\mathbf{r}_i - \mathbf{r}_j)^2 \right] + \sum_{i<j<k}^{A} V_{NNN}^{ijk}, \tag{3}$$

and $H_{\text{CM}} = \mathbf{P}^2/2mA + mA\Omega^2\mathbf{R}^2/2$ is the center-of-mass term.

Shell-model calculations are carried out in a model space defined by a projector P. The complementary space to the model space is defined by the projector $Q = 1 - P$. With the above Hamiltonian, we can then construct an effective interaction acting within the model space P, reproducing exactly N_P eigenvalues of the full Hamiltonian. This can be accomplished by a similarity (Lee-Suzuki) transformation [91–94]. However, no

unique unitary transformation exists: one can construct infinitely many different unitary transformations which decouple the model and complementary ($Q = 1-P$) subspaces, as discussed in Ref. [95]. Calculation of the exact A-body effective interaction is, however, as difficult as finding the full space solution. Using two-body interactions, the effective interaction is often approximated by a two-body effective interaction determined from a two-nucleon subsystem.

The above-mentioned transformation can be performed also in a three-nucleon space. This will generate effective 3NFs even if the starting Hamiltonian includes only two-body terms. These effective interaction calculations are performed in a Jacobi coordinate HO basis [39, 96]. An effective three-body interaction can be computed also for starting Hamiltonians with pure NN interaction terms. This procedure has been shown to speed up convergence [96], although it should be noted that all cluster-approximated effective interactions ($a < A$) will in this approach reproduce the free interaction results in the infinite model space limit.

2.2.2. Similarity transformed effective interactions in momentum space   Alternatively, instead of carrying out the similarity transformation in an oscillator basis, one can perform the transformation in momentum space [97]. This approach consists of two steps: (i) a diagonalization of the two-body Schrödinger equation in the full momentum space, and (ii) a similarity transformation [93, 94] to relative momenta $k \in [0, \Lambda]$ fm^{-1}, with Λ defining the relative momenta model space. Typical values of Λ are in the range of ~ 2 fm^{-1}. This evolution to lower k-values can be performed using renormalization group (RG) methods [98, 99]. We note, however, that the RG approach differs from the Lee-Suzuki transformation as the Q-space block of the effective Hamiltonian is now set to zero. The evolution to lower cutoffs shifts contributions from the sum over intermediate states to the interactions, just as RG equations in quantum field theory shift strength from loop integrals to coupling constants. The evolved low-momentum effective NN interactions have been dubbed $V_{\mathrm{low}-\mathrm{k}}$ [97]. These interactions are significantly softer; hence, more perturbative, as seen, e.g., in nuclear matter calculations [100]. By construction, $V_{\mathrm{low}-\mathrm{k}}$ preserves two-nucleon observables for relative momenta up to the cutoff. It should be noted, however, that no tractable approach to evolve many-body forces in this approach has been proposed so far.

2.2.3. Similarity renormalization group transformed interactions   In recent years, a new approach to perform the similarity transformation has been developed and used, in particular, with the chiral interactions. The similarity renormalization group (SRG) approach [101, 102] builds on the general principle of RG theory, namely that the relevant details of high-energy physics for calculating low- energy observables can be captured in scale-dependent coefficients of operators in a low-energy Hamiltonian. Using this principle as a guide, the transformed Hamiltonian $H_s = U_s^{\dagger} H U_s$ can be expressed

through a differential (flow) equation

$$\frac{dH_s}{ds} = [\eta_s, H_s] \,, \tag{4}$$

in which η_s is the generator of the flow, an antihermitian operator that is related to the unitary transformation at the resolution scale s through

$$\eta_s \equiv \frac{dU_s}{ds} U_s^\dagger \equiv -\eta_s^\dagger. \tag{5}$$

The evolved Hamiltonian is $H_s \equiv T_{\rm rel} + V_s$, where the s-dependence is contained fully in the effective potential V_s. The crucial step of the method is the choice of the most appropriate generator η. The antihermitian property is automatically fulfilled by

$$\eta_s = [G_s, H_s] \,, \tag{6}$$

where G_s is a momentum-diagonal operator. With this choice, the transformed operator flows towards a band-dagonal form in momentum space, thus achieving the desired decoupling property. Applications to nuclear forces have used $G_s = T_{\rm rel}$ [97, 103].

We should note that the generator of the flow is a many-body operator, which implies that it induces many-body terms in the effective operator, see Sec. 3.1. In principle, the evolution of many-body forces is straightforward, which is an advantage of the SRG method. However, the associated technical difficulties are significant. While the two-body evolution is usually performed in momentum space [103], the three-body evolution was first implemented in a three-body HO basis [104, 105]. A first implementation of the SRG flow equation in three-body momentum space was first performed for a one-dimensional model [106] and, more recently, for realistic chiral interactions [107].

Finally, we want to highlight an important difference between the Lee-Suzuki transformation and the scale-dependent effective interactions discussed in Secs. 2.2.2 and 2.2.3. While the Lee-Suzuki transformation also induces many-body terms it will, by construction, reproduce the bare-interaction results already in a two-body cluster approximation (i.e., without induced many-body forces) – as the many-body space is extended towards the full Hilbert space. This property is not shared by the SRG and $V_{\rm low-k}$ effective interactions. By truncating the flow at two- or three-body level, the unitarity of the transformation is violated, and the bare result will not be reproduced, even when the many-body model space becomes the full Hilbert space.

2.3. Configuration interaction and coupled cluster theory

Present shell-model codes can reach dimensions of $d \sim 10^{10}$ basis states [38, 84, 108, 109], and Monte Carlo-based shell-model codes can attack problems with $d \sim 10^{15-16}$ [26, 27, 110–112]. Although these numbers are impressive, the dimension limitation has important implications for calculations of nuclei that involve weakly bound states and/or resonances, as such states require still larger basis sets. Extensions of the NCSM to weakly bound systems will be discussed below.

Large-scale diagonalization is widely used in many areas of physics, from quantum chemistry [23] to nuclear physics [38]. The method is based on a projection of the model Hamiltonian onto a finite-dimensional subspace of the many-body Hilbert space; hence, the method is an instance of the Rayleigh-Ritz method. In the standard-shell model approach, one takes the stance that the many-body Hamiltonian is composed of two parts: $\hat{H}_0$ and $\hat{H}_I$, treating the latter as a perturbation of the former. The eigenfunctions of the mean-field Hamiltonian, $\hat{H}_0$, are assumed to comprise a single-particle basis for the Hilbert space. This leads to a matrix diagonalization problem, hence the name of the method. As $\hat{H}_I$ is the residual interaction that "perturbs" simple configurations of $\hat{H}_0$, the method is commonly referred to as the configuration-interaction method.

The NCSM method differs from the standard shell model in several ways: (i) there is no core, which implies that all nucleons are included in the many-body basis; (ii) no mean field is introduced and all interactions are included explicitly; (iii) the center-of-mass motion is separated exactly; and (iv) NCSM Hamiltonian contains realistic two- and three-body nuclear interactions and the Hamiltonian matrix is usually built from these interactions using the similarity transformations.

Coupled cluster theory employs a different approach to systematically build the many-body wave functions using a large number of single-particle states. In actual calculations one typically limits the number of active many-body states to at most three-particle-three-hole excitations, whereas the single-particle basis can easily be extended to some 20 major oscillator shells. This has important consequences for studies of weakly bound systems. The coupled-cluster method has a rich history in both nuclear physics [113–116] and quantum chemistry [23, 117].

In this contribution we highlight recent achievements and important lessons learned from *ab initio* calculations performed with the NCSM and coupled-cluster methods. In the following, we outline the essential features of these two approaches.

2.3.1. No-core shell-model theory The starting point for NCSM calculations is the translationally invariant Hamiltonian H of Eq. (1). This Hamiltonian is however modified by adding a HO center-of-mass Hamiltonian $H_{\mathrm{CM}} = T_{\mathrm{CM}} + U_{\mathrm{CM}}$, where $U_{\mathrm{CM}} = Am\Omega^2\mathbf{R}^2/2$. In practice, the Hamiltonian $H + H_{\mathrm{CM}}$ is used as input to the computation of a similarity transformed effective interaction. At the stage of constructing the many-body Hamiltonian matrix, the HO center-of-mass term is subtracted and a Lawson projection term $\beta\left(H_{\mathrm{CM}} - \frac{3}{2}\hbar\Omega\right)$ is added to shift spurious CM excitations up in the energy spectrum.

The truncation of the many-body model space is usually performed in terms of the total energy. That is, the sum of HO excitations that is contained in a Slater determinant basis state is restricted according to $\sum_i^A (2n_i + l_i) \leq N_{\mathrm{tot,max}}$. More often, however, the basis truncation is specified in terms of N_{max} that measures the total number of HO excitations above the unperturbed ground state. For $A = 3, 4$, these two measures are the same, but for *p*-shell systems they differ, e.g., for ^{6}Li, $N_{\mathrm{max}} = N_{\mathrm{tot,max}} - 2$, and for ^{11}Li, $N_{\mathrm{max}} = N_{\mathrm{tot,max}} - 7$, etc. As an example, the ^{6}Li results that are presented in

Sec. 3.1 were obtained in model spaces up to $N_{\max} = 16$. With this $N_{\max}$-truncation, the highest single-particle state that can be reached has the energy $(2n + l)\hbar\Omega = 17\hbar\Omega$, which gives 171 possible nlj orbitals and 2280 individual single-particle states ($nljm$). The dimension of the many-body space is $d = 0.79 \cdot 10^9$. This Hamiltonian matrix is very sparse and can be diagonalized using iterative Lanczos algorithms for real, symmetric matrices [118]. The ground-state is usually reached with $10 - 20$ Lanczos iterations. The method provides excitation spectra as well as wave functions, from which various observables can be computed.

Since NCSM employs HO basis and the total energy truncation (including *all* allowed configurations), any eigenstate of the translationally invariant Hamiltonian factorizes into a product of a wave function depending on intrinsic coordinates, and a wave function depending on the center-of-mass coordinate. The use of any other single-particle basis, or any other truncation scheme, results in a mixing of intrinsic and center-of-mass motions.

Several important ingredients are not considered here, such as the construction of antisymmetric, few-body states in the Jacobi-coordinate basis needed for the computation of interaction matrix elements. For the many-body systems considered here, the antisymmetric many-body states are constructed in the uncoupled M-scheme. For a much more complete description of the NCSM method, see Ref. [39].

2.3.2. Coupled cluster theory The single-reference coupled cluster theory is based on the exponential ansatz for the ground-state wave function of the A-nucleon system,

$$|\Psi_0\rangle = e^T|\Phi_0\rangle, \tag{7}$$

where $|\Phi_0\rangle$ is an uncorrelated, closed shell reference state, and T is a linear expansion in particle-hole excitation amplitudes.

The approximation that is made in the coupled-cluster approach is the truncation of the correlation operator T at a given (low-order) particle-hole excitation level. Note that in contrast to the full configuration interaction method, where the expansion in particle-hole excitation amplitudes is linear, the expansion is non-linear in the coupled-cluster approach due to the exponentiation of T. The most commonly used approximation in the coupled-cluster approach is the truncation of the operator T at the singles-and doubles excitation level (CCSD). Higher accuracy can be obtained by including triples excitations (CCSDT) [22, 117]. In terms of computational cost, the CCSD method scales as $n_o^2 n_u^4$, while the full CCSDT scales as $n_o^3 n_u^5$, where n_0 represents the number of occupied orbitals and n_u the number of unoccupied single-particle states. Since coupled cluster theory with inclusion of full triples CCSDT is usually considered to be too computationally expensive, several approximations to the solution of the CCSDT equations have been developed. A sophisticated way of approximating CCSDT is known as the Λ-CCSD(T) approach [119, 120], in which the left-eigenvector solution of the CCSD similarity-transformed Hamiltonian is utilized in the calculation of a non-iterative triples correction which scales as $n_o^3 n_u^4$. Excited states and neighbors of closed

shell nuclei can be computed within the equation-of-motion methods [117]. Recently, the coupled-cluster method in an angular momentum coupled scheme was developed in Ref. [24, 121]. This allows to address medium mass and neutron rich nuclei starting from "bare" chiral interactions. Results presented in this contribution will focus on the CCSD and the Λ-CCSD(T) approach, with various equation-of-motion methods for open-shell nuclei and excited states [24, 122].

2.4. Theoretical treatment of open systems

As discussed earlier, the description of loosely bound and unbound nuclear states represents a challenge for nuclear structure models [123]. Several approaches to this problem are based on the use of the so-called Berggren basis [49–51]. Modern applications of the continuum shell model include the (real-energy) Shell Model Embedded in the Continuum [124–127] based on the Feshbach projection formalism [128], and the (complex energy) GSM [48,129–131] employing the Berggren basis [49–51]. The Berggren completeness relation can be written as:

$$\sum_{n=b,d} |\tilde{u}_n\rangle\langle u_n| + \int_{L^+} dk|\tilde{u}_k\rangle\langle u_k| = 1, \tag{8}$$

where b are bound states, d - decaying resonant states, and the integral along a contour L^+ in the complex-k plane represents the contribution from the non-resonant scattering continuum, see Fig. 2. In general, different contours can be used for different (ℓ, j) partial waves.
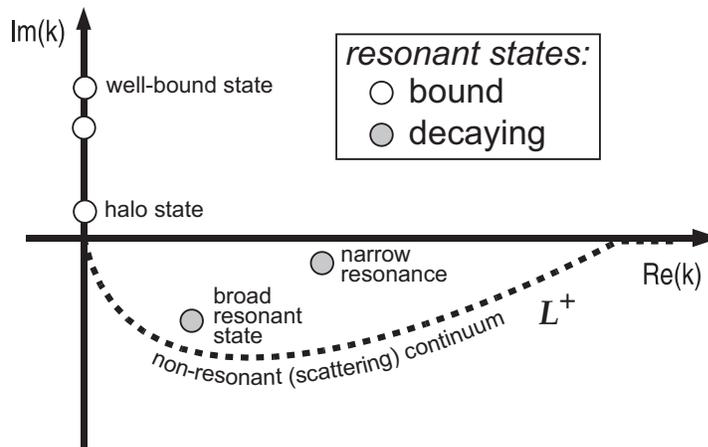
Figure 2. Illustration of the Berggren completeness relation (8) in the complex k-plane. The bound states are located on the positive imaginary axis. The weakly bound halo states lie close to the origin. The positive-energy resonant states are located in the fourth quadrant. Those with a small imaginary part can be interpreted as resonances. The complex-k contour L^+ represents the non-resonant scattering continuum.

The recent GSM applications include the analysis of threshold effects in multichannel coupling and spectroscopic factors [132, 133], description of isospin mixing

in weakly bound nuclei [134], explanation of behavior of charge radii in helium halo nuclei [135], and studies of asymptotic normalization coefficients in mirror nuclei [136]. Another exciting development utilizing the Berggren basis is the extension of the coupled-cluster method to open systems; it represents the first complex-energy nuclear *ab initio* framework [45, 53, 87] capable of describing many-body bound and unbound states. In actual coupled-cluster calculations, one performs first a Hartree-Fock calculation and transforms the Hamiltonian to the Hartree-Fock basis. As a consequence, the coefficients t_i^a of the singles amplitude, see Sec. 2.3.2, acquire small values in the solution of the coupled-cluster equation. One also finds, when using a HO basis, that this approach reduces the $\hbar\Omega$-dependence of the computed energies. In practical computations one aims at increasing the number $N+1$ of employed oscillator shells until the results become virtually independent on the model-space parameters. In Ref. [52] it was demonstrated that one could start with a standard HO basis and corresponding interactions. We refer the reader to the latter reference for further details.

In order to use the Berggren basis in large-scale configuration-mixing calculations, the integral over the non-resonant continuum is discretized by using a suitable quadrature rule. Using this discrete Berggren basis, the GSM basis is obtained in the usual way by constructing many-body Slater determinants. The dimension of the Hamiltonian matrix grows rapidly with the number of discretized continuum states and the number of nucleons; hence, advanced numerical methods that can handle large non-Hermitian matrices must be used. In the context of the GSM, it has been shown that the Density Matrix Renormalization Group (DMRG) is an efficient way to compute the low-lying spectrum of the Hamiltonian at a low computational cost.

2.4.1. Density Matrix Renormalization Group for the GSM The DMRG method was first introduced to overcome the limitations of the Wilson-type renormalization group to describe strongly correlated systems with short-range interactions [32, 137]. More recently, the DMRG has been reformulated and applied to finite Fermi systems [138], nuclear shell model [139–141], and open systems [142]. While most of the DMRG studies have been focused on properties in strongly correlated closed quantum systems characterized by Hermitian density matrices, systems involving non-Hermitian and non-symmetric density matrices can also be treated [34, 142, 143].

Let us consider the application of the J-scheme DMRG in the context of the GSM (GSM+DMRG). The objective is to calculate an eigenstate $|J^\pi\rangle$ of the GSM Hamiltonian $\hat{H}$ with angular momentum J and parity π. As $|J^\pi\rangle$ is a many-body pole of the scattering matrix of $\hat{H}$, the contribution from non-resonant scattering shells along the continuum contour L^+ to the many-body wave function is usually smaller than the contribution from the resonant orbits [48]. Based on this observation, the following separation is usually performed [142]: the many-body states constructed from the single-particle poles form a subspace A (the so-called 'reference subspace'), and the remaining states containing contributions from non-resonant shells form a complement subspace B (see Fig. 3).
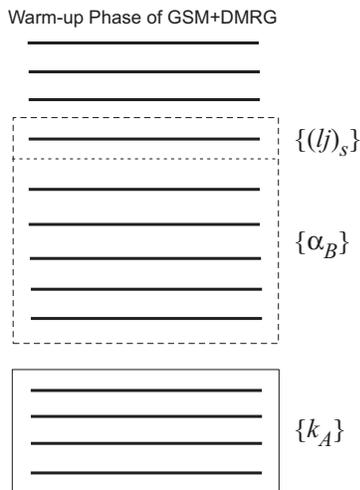
Warm-up Phase of GSM+DMRG

$\{(lj)_s\}$

$\{\alpha_B\}$

$\{k_A\}$

Figure 3. Schematic illustration of the GSM+DMRG procedure during the sth step of the warm-up phase. States $\{k_A\}$ from A, previously optimized states α_B, and states $\{(lj)_s\}$ constructed by occupying the sth shell with n particles are coupled to generate the new set of states $\{k_A \otimes i_B\}^J = \{k_A \otimes \{\alpha_B \otimes (lj)_s^n\}\}^J$.

One begins by constructing states $|k\rangle_A$ forming the reference subspace A. All possible matrix elements of suboperators of the GSM Hamiltonian $\hat{H}$ acting in A, expressed in the second quantization form, are then calculated and stored and the GSM Hamiltonian is diagonalized in the reference space to provide the zeroth-order approximation $|\Psi_J\rangle^{(0)}$ to $|J^\pi\rangle$. This vector, called 'reference state', plays an important role in the GSM+DMRG truncation algorithm. The scattering shells (lj), belonging to the discretized contour L^+, are then gradually added to the reference subspace to create the subspace B. This first stage of the GSM+DMRG procedure is referred to as the 'warm-up phase. For each new shell that is added, all possible many-body states denoted as $|i\rangle_B$ are constructed and matrix elements of suboperators of the GSM Hamiltonian acting on $|i\rangle_B$ are computed. By coupling states in A with the states $|i_B\rangle$, one constructs the set of states of a given J^π. This ensemble serves as a basis in which the GSM Hamiltonian is diagonalized. The target state $|\Psi_J\rangle$ is selected among the eigenstates of $\hat{H}$ as the one having the largest overlap with the reference vector $|\Psi_J\rangle^{(0)}$. Then, the desired truncation is performed in B by introducing the reduced density matrix, constructed by summing over the reference subspace A [144]. In standard DMRG applications for Hermitian problems, where the eigenvalues of the density matrix are real non-negative, only the eigenvectors corresponding to the largest eigenvalues are kept during the DMRG process. Within the metric defining the Berggren ensemble, the GSM density matrix is complex-symmetric and its eigenvalues are, in general, complex. As a consequence, the truncation is done by keeping the eigenstates α_B (the 'optimized' states) with the largest nonzero moduli of eigenvalue [34].

The warm-up phase is followed by the so-called sweeping phase, in which, starting from the last scattering shell $(lj)_{\text{last}}$, the procedure continues in the reverse direction

(the 'sweep-down' phase) until the first scattering shell is reached. The procedure is then reversed and a sweep in the upward direction (the 'sweep up' phase) begins. The sweeping sequences continue until convergence for target eigenvalue is achieved.

Applications of GSM+DMRG have been reported in Refs. [34, 135, 142]. Those examples demonstrate that weakly-bound and unbound nuclear systems, which – because of a prohibitively large size of Fock space, cannot be treated by means of direct diagonalization techniques – can be treated very efficiently using DMRG. The DMRG also opens up the avenue to perform NCSM calculations for open systems using the Berggren basis [54].

2.4.2. The Resonating Group Method An alternative formulation for describing open quantum systems, characterized by a limited number of open channels, is the resonating group method (RGM) [145]. Here, the many-body wave function is decomposed into contributions from various channels that are distinguished by their different arrangement of the nucleons into clusters. In principle, this corresponds to the expansion of the bound state, or the interior region of a scattering state, into an over complete set of basis functions. The basis functions consist of two parts: the cluster wave functions and the wave function representing the relative motion of the clusters. In the case of two clusters, for instance, the full wave function of the system can be written as

$$\Psi^{(A)} = \sum_{\nu} \mathcal{A}_{\nu} \left\{ \Phi_{1\nu} \Phi_{2\nu} \varphi_{\nu}(\vec{r}_{\nu}) \right\}, \tag{9}$$

where ν labels cluster channels. This expansion is complicated due to the presence of the antisymmetrizer $\mathcal{A}_{\nu}$, which accounts for the exchange of nucleons between the clusters. The intrinsic wave functions, $\Phi_{1,2}$, are internally antisymmetric and would, in the NCSM+RGM approach [146, 147], be eigenstates of the NCSM Hamiltonian for that particular cluster.

At this point, a basis of binary-cluster channel states, $|\Phi_{\nu r}^{J^{\pi}T}\rangle$, is introduced that includes the spin-coupled product of internal (antisymmetric) wave functions of the two clusters at relative distance r. This basis can be used to expand the many-body wave function:

$$|\Psi^{J^{\pi}T}\rangle = \sum_{\nu} \int dr \, r^2 \frac{g_{\nu}^{J^{\pi}T}(r)}{r} \, \hat{\mathcal{A}}_{\nu} \, |\Phi_{\nu r}^{J^{\pi}T}\rangle. \tag{10}$$

By diagonalizing the NCSM Hamiltonian in this basis, one obtains the RGM equations:

$$\sum_{\nu} \int dr \, r^2 \left[\mathcal{H}_{\nu'\nu}^{J^{\pi}T}(r', r) - E \, \mathcal{N}_{\nu'\nu}^{J^{\pi}T}(r', r) \right] \frac{g_{\nu}^{J^{\pi}T}(r)}{r} = 0, \tag{11}$$

where $\mathcal{N}_{\nu'\nu}^{J^{\pi}T}(r', r)$ and $\mathcal{H}_{\nu'\nu}^{J^{\pi}T}(r', r)$ are the norm and Hamiltonian kernels, respectively. These non-local quantities contain all the nuclear structure information. However, we note that the basis states are asymptotically orthogonal so that all important physical quantities (such as the scattering matrix) can be defined with the asymptotic solution. The non-orthogonality mainly appears at short distances and is primarily

due to antisymmetrization effects. The RGM equations can be solved by means of the standard symmetric orthogonalization method [147].

The NCSM+RGM approach has been initially used for single-nucleon projectiles, both for scattering and bound-state cases [146–148]. The method has recently been extended to study projectile-target binary-cluster states, where the projectile is a deuteron [149]. This new development makes it possible to compute, e.g., $d+^4$He scattering, clusterized ^{6}Li states, as well as deuteron fusion reactions on ^{3}H and ^{3}He [150].

3. Selected results

In this section, we focus on selected results for several chains of neutron-rich isotopes, both light and heavy. We base our theoretical analyses on large-scale NCSM calculations, coupled-cluster calculations, and nuclear DFT. An important question is the role played by three or more complicated many-body terms in the low-energy effective nuclear Hamiltonian. The study of 3NFs in medium mass and neutron rich nuclei is an ongoing research topic in nuclear many-body physics. Several calculations indicate that 3NFs are needed to understand various properties of nuclei, see for example Refs. [39, 42, 45, 46, 80, 84, 85, 87, 105]. As one moves to more neutron-rich isotopes, correlations play an increasingly more important role. The mean field contribution is often reduced relatively to the effects due to two-, three- and many-body correlations. Furthermore, close to the drip lines, the number of degrees of freedom increases dramatically, with resonant and non-resonant continuum channels becoming available. All of this requires a good understanding of correlations and interactions driving the observed properties.

A three-body force is expected to play a role in the evolution of single-particle energies as more and more particles are added. For instance, the effect of the monopole term has been analyzed intensively in terms of phenomenological interactions over the last two decades [38, 151–153]. However, there is also clear evidence from several calculations that a traditional shell-model picture with a strong mean field that defines a single-particle basis, may break down, see for example Refs. [21, 87] and discussion below.

As outlined in this contribution, we are now in a position where 3NFs from EFT can be included routinely into various *ab initio* methods. This means that we can start to explore, which components of the nuclear forces are at play when we move towards the drip lines. Furthermore, with long chains of isotopes to be studied theoretically and experimentally, one can eventually attempt to extract in-medium information that will allow us to constrain 3NFs for heavier nuclei.

In the following, selected results for light and medium-heavy are discussed. We shall focus on results for binding energies and a few excited states for selected chains of isotopes In several cases we will study the impact of 3NFs and couplings to the continuum.

3.1. Results for light nuclei

In this section, we mainly focus on *ab initio* description of light nuclei near the drip lines. We shall restrict discussion to approaches that try to solve the many-body Schrödinger equation without uncontrolled approximations, using a well-defined microscopic Hamiltonian as a single input. While there are several realistic nuclear interactions that reproduce NN scattering phase shifts and few-body data with high precision, we focus mainly on results obtained with chiral interactions.

Bound state *ab initio* calculations of light nuclei were pioneered by the Variational Monte Carlo (VMC) and Green's Function Monte Carlo (GFMC) methods [25]. They have studied $A = 4 - 12$ systems using various combinations of Argonne NN interactions and UIX or Illinois (IL) 3NFs, and have demonstrated an impressive agreement with experimental energies, not only for bound states but also for narrow resonances [154].

Ab initio methods that can currently model systems with $A > 4$, include the Effective Interaction for Hyperspherical Harmonics (EIHH) [155, 156], lattice calculations [80, 157], the coupled-cluster method [24, 116, 158], and the No-Core Shell Model [39, 44, 159]. The EIHH is currently limited to $A \leq 6$ due to the difficulty of antisymmetrization. Calculations on the lattice for light bound systems [157] and the Hoyle state [80] have been recently reported.

As a benchmark example, and an illustration of the use of modern chiral interactions including consistent 3NFs in NCSM, we present in Table 1 results for $A = 3, 4$ obtained

Table 1. Properties of ^{3}H and ^{4}He. Benchmarking of calculations with chiral NN+3NF interactions using NCSM [160] and Hyperspherical Harmonics [161] methods. (From Refs. [39, 162].)

		NN (N^{3}LO)		+3NF(N^{2}LO)		Expt.
		NCSM	HH	NCSM	HH	
^{3}H	E_{gs} [MeV]	7.852(5)	7.854	8.473(5)	8.474	8.482
	$\langle r_p^2 \rangle^{1/2}$ [fm]	1.650(5)	1.655	1.608(5)	1.611	1.60
^{4}He	E_{gs} [MeV]	25.39(1)	25.38	28.34(2)	28.36	28.296
	$\langle r_p^2 \rangle^{1/2}$ [fm]	1.515(2)	1.518	1.475(2)	1.476	1.467(13)

with and without inclusion of 3NFs. The chiral 3NF is from order N^{2}LO and contains two low-energy constants (LEC) that need to be determined from $A > 2$ data. In Ref. [160], these constants were obtained from $A = 3$ binding energies, but also by investigating sensitivities of properties of $A \geq 4$ nuclei to the variation of the constrained LECs. Besides the triton ground state energy, which is by construction within a few keV of experiment, the NN+3NF results for the ^{4}He ground-state energy and point-proton radius are in excellent agreement with measurement. We also note a very good agreement between NCSM and the variational HH method [161].

Developments based on an importance-truncation (IT) have recently been proposed in Ref. [163] to address the factorial growth of the NCSM model space with N_{max} and

particle number A. With a criterion based on perturbation theory, a large fraction of the many-body basis states can be discarded and calculations with $N_{\max} = 12$ for ^{12}C and ^{16}O have become feasible [105].

Let us first consider the chain of He isotopes. The charge radii and masses of He isotopes (up to ^{8}He) were recently determined experimentally [164,165] and compared to results from *ab initio* methods. For ^{6}He in particular, results for radii and binding energies are available from calculations with GFMC [166], NCSM [167], FMD [168], and EIHH [165,169]. Unfortunately, at the present stage, those results can not be used for benchmarking as different interactions have been used. Actually, the GFMC results are the only published converged calculations that include 3NFs. Within the range of GFMC results, it is possible to reproduce both the charge radius and separation energy. However, there is a large uncertainty due to different models of 3NFs and different trial wave functions used.

The first *ab initio* coupled-cluster calculations using a Berggren basis were performed in Ref. [170]. Within the coupled cluster singles-and-doubles approximation (CCSD), the ground state binding energies and lifetimes of the $^{3-10}$He isotopes were calculated employing V_{low-k} with cutoff $\Lambda = 1.9\text{fm}^{-1}$, derived from the N^{3}LO nucleon-nucleon interaction of Ref. [81]. A comparison between the CCSD results and experiment is shown in Fig. 4 and demonstrates a fair agreement. An improved description of the helium isotopes must include the effects of 3NFs and triples correlations (CCSDT).
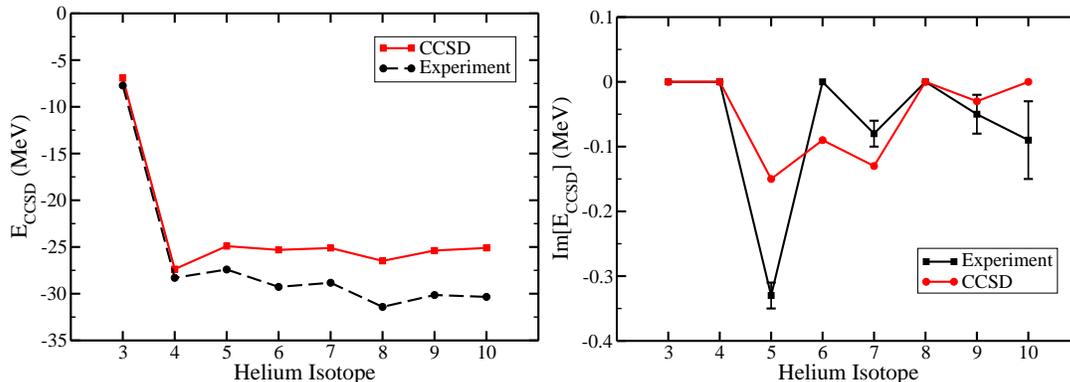
Figure 4. Left panel: CCSD ground state energies (red solid line) compared to experimental binding energies (black dashed line) for $^{3-10}$He. Right panel: Imaginary parts of the CCSD (red solid line) and experimental (black dashed line) ground state energies for $^{3-10}$He.

A hallmark feature of halo systems appearing near the nucleon drip line is the rapid increase of matter radii. Corresponding effects on the charge radius are much smaller, but this quantity can be studied very accurately using laser spectroscopy techniques. Let us consider the neutron-rich nuclei ^{6,8}He as an example. The charge radius of ^{6}He is 2.059(7) fm and exceeds that of ^{8}He, which is 1.959(16) fm, see Refs. [164,165]. Both of them are much larger than the charge radius of ^{4}He, 1.681(4) fm. These two heavy

helium isotopes are neutron halo nuclei and, since the protons are confined inside the tightly bound α-core, the differences of charge radii carry unique structural information on the nuclear Hamiltonian and many-body dynamics. In Ref. [135], ^{6}He and ^{8}He were described with the GSM as systems of valence neutrons moving outside the α core, and interacting via a finite-range Minnesota potential. The core-neutron potential was described by a Woods-Saxon potential and the model space was constructed from the Berggren basis. While such a calculation is obviously not not *ab initio*, it allows us to understand intricate experimental data in simple terms. Specifically, the GSM work demonstrated that the observed charge radii depend mainly on three factors: (i) the recoil due to the motion of valence nucleons around the α-core; (ii) the spin-orbit term; and (iii) the swelling of the α-core in the neutron environment (see Fig. 5). While (i) and (ii) are robustly predicted by GSM (i.e., they depend weakly on the interaction, provided that the threshold energies are under control), the core swelling effect (iii) must be taken from an *ab initio* theory (here, from GFMC calculations [166]). One can thus conclude that the GSM approach links the high-quality atomic data to a subtle in-medium effect that provides a stringent test of *ab initio* theory.
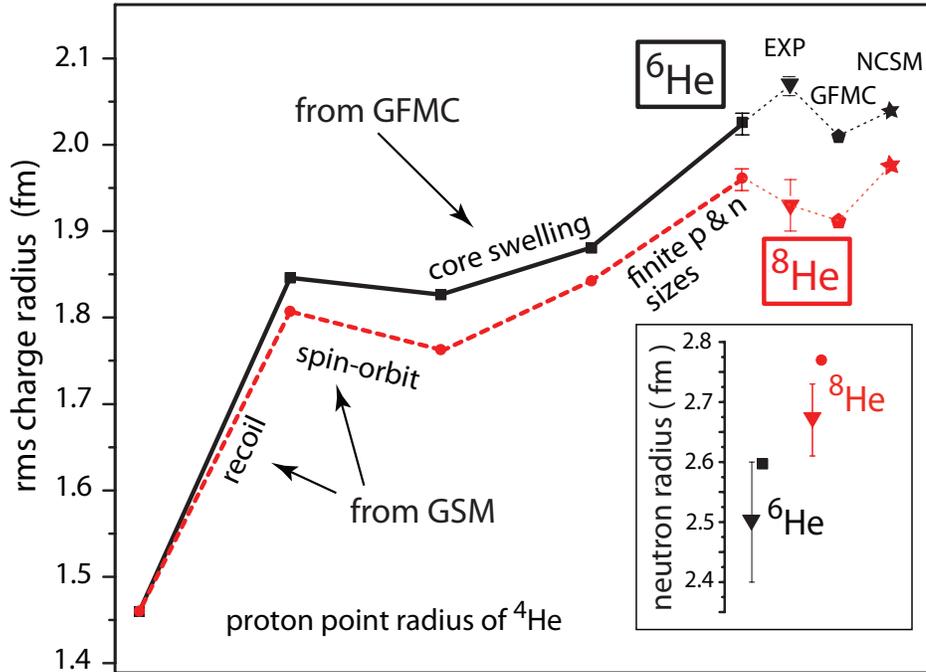
Figure 5. Different contributions to the charge radius of ^{6}He (solid line, squares) and ^{8}He (dashed line, dots) calculated in GSM. The core swelling contribution is taken from GFMC calculations of Ref. [25]. Experimental charge radii come from [165] (triangles). The NCSM [167] (stars) and GFMC [166] (pentagons) results are marked for comparison. The inset shows GSM rms neutron radii compared to experiment [171]. (From Ref. [135].)

The chain of lithium isotopes offers many splendid examples of drip line physics. The nucleus ^{6}Li belongs to the valley of beta-stability and ^{7,8,9}Li are particle-bound but

beta-unstable. Adding one more neutron to ^{9}Li yields an unbound ^{10}Li, while adding a pair of neutrons produces the additional pairing energy that makes ^{11}Li bound. Such an even-odd staggering effect in binding energy can be often seen along the neutron drip line. The conventional shell model picture of ^{11}Li puts the valence neutrons in a p-wave state. However, measured angular correlations in fragmentation reactions [172] demonstrate the presence of states with different parities. Furthermore, the structure of the unbound ^{10}Li is expected to correspond to a virtual s-state with a very large scattering length. These phenomena: melting and re-organizing of shell structure, ground states embedded in the continuum, and dilute matter densities such as halos, appear in most isotopes around the drip lines. They just illustrate a point that will be made clear throughout this contribution, namely, light nuclei living on the edge of stability cannot be described within a mean-field picture.

The Li and Be isotopic chains were recently studied in the NCSM [173] to investigate the wealth of exotic properties that generally pose a challenge for nuclear-structure models: (i) appearance of clustering; (ii) halo structure of ^{11}Li; and (iii) low ground-state quadrupole moment of ^{6}Li. In this systematic study, series of calculations were carried out in large model spaces using CD-Bonn 2000 [74], and INOY (IS-M) [174] interactions. The degree of convergence was estimated from the $N_{\max}$- and $\hbar\Omega$-dependence of the results. Alternatively, one can utilize the fact that NCSM calculations performed at different HO frequencies should all converge to the same value in the limit $N_{\max} \to \infty$. This constitutes an example of multiple converging sequences in the NCSM, discussed extensively in Ref. [175]. In this context, we note that much work is currently focused on quantifying the basis truncation corrections [14, 176].

Figure 6 shows the ground-state energies of $A = 6 - 11$ Li isotopes. The isotopic trend is nicely reproduced, but also the known feature of pure NN interactions giving too little binding for many-nucleon systems is seen. The INOY interaction is a bit different as the NN P-wave scattering has been modified slightly in order to reproduce binding energies and the analyzing powers in the $A = 3$ systems. Note that the model spaces used in computations of ^{11}Li were not large enough to reach the exponential convergence region.

In Fig. 7 we compare the calculated and experimental trends for a number of observables for the Li chain of isotopes. With the important exception of the radius of the ^{11}Li halo ground-state, a good agreement between NCSM results and experiment is found. In particular, the overall trends are well reproduced. In this context, however, it is important to point out that calculations of electromagnetic moments are usually performed in the impulse approximation (i.e., one-body nucleon currents), and that the inclusion of meson exchange currents can add about 20% to magnetic dipole moments [177]. We expect more work in this direction, including fully consistent two-body currents from chiral Lagrangians. Another success of NCSM calculations, is the reproduction of the small quadrupole moment of ^{6}Li that is known to pose a challenge for theory. In particular, the general failure of three-body models for this observable has been blamed on missing antisymmetrization of the valence nucleons and the nucleons in
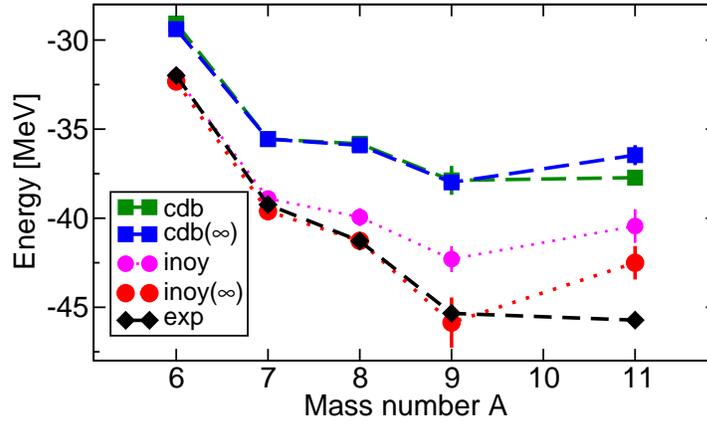
Figure 6. Ground-state energies for Li isotopes predicted in NCSM compared with experiment. The exponential convergence rate was not fully reached for ^{11}Li. (From Refs. [162, 173].)
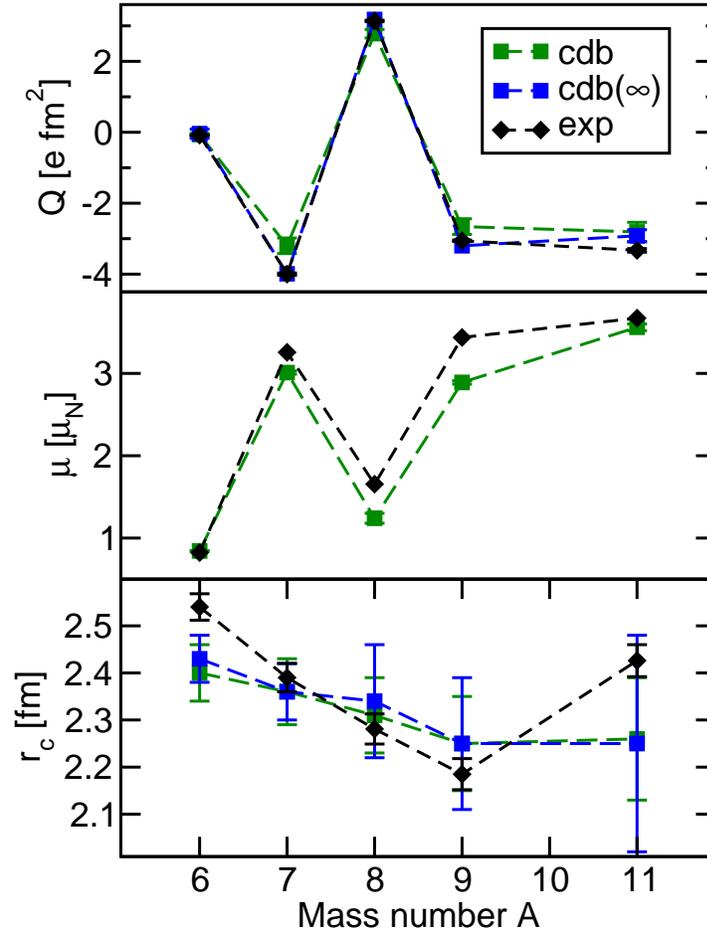

Figure 7. Electric quadrupole moments, magnetic dipole moments, and charge radii of Li isotopes obtained in NCSM and compared with experiment. (From Refs. [162,173].)

the alpha-core [178]. In addition, the ratio $Q\left(^{11}\text{Li}\right)/Q\left(^{9}\text{Li}\right)$ is found to be very close to

unity, as confirmed by very precise experimental data [179], and the trend for the much larger moments of $A = 7 - 11$ is nicely reproduced. This has been obtained within the truncated HO basis space that does not give a very accurate description of the dilute halo structure of ^{11}Li. Still, the observed decrease of the charge radius in $A = 6 - 9$ is reproduced.

A clear example of the disappearance of magic numbers in weakly bound systems is found in ^{11}Be. The experimental ground state of ^{11}Be is an intruder $1/2^+$ level, while the first p-shell state is $1/2^-$ situated at $E_x = 320$ keV. The neutron separation energy is only 503 keV, and there are no other bound states. An investigation of $A = 9, 11$ isotopes in large-basis *ab initio* NCSM calculations were reported in Ref. [180]. Calculations were performed for both natural-parity and unnatural-parity states in model spaces up to $N_{max} = 9$ using four different accurate NN potentials. The ^{11}B $N_{max} = 9$ calculation, with a basis dimension of $1.1 \cdot 10^9$, was the largest NCSM diagonalization at that time. The calculations did not reproduce the anomalous $1/2^+$ ground state, but did predict a dramatic drop in the positive-parity excitation energies with an increasing model space. Furthermore, the behavior of the INOY results suggested that a realistic NNN force might have an influence on the observed parity inversion.

It is expected that the halo character of a loosely bound neutron should have a major influence on the characteristics of a nuclear state. This fact is illustrated by the extremely strong E1 transition between the two bound states in ^{11}Be, that can be explained by a large overlap of the initial and final state wave functions at large distances. The E1 strength was underestimated by a factor of 20 in the NCSM calculations [180], demonstrating that the halo character of this state is extremely hard to reproduce using a HO basis. This observation makes ^{11}Be an excellent candidate for testing the NCSM+RGM method, in which the relative motion of the core and the valence nucleon is treated more accurately. By imposing bound-state boundary conditions to the set of coupled channel Schrödinger equations of Eq. (11), the bound states of ^{11}Be could be studied in a NCSM+RGM model space spanned by the $n+^{10}$Be channel states with inclusion of the ground state plus three excited states of ^{10}Be [146]. Binding energies of the various ^{10,11}Be states are displayed in Table 2 for both NCSM and NCSM+RGM. The precise treatment of the neutron halo strongly influences the S-wave relative kinetic and potential energies. The rescaling of the relative wave function in the internal region, seen in the NCSM+RGM, is the main cause of the dramatic decrease (~ 3.5 MeV) of the energy of the $1/2^+$ state. This effect makes the $1/2^+$ state bound and even leads to a parity inversion in NCSM+RGM.

Let us mention also modern nuclear reaction calculations that offer opportunities to compute new observables that probe other properties of realistic nuclear Hamiltonians. Here we present results from $N + \alpha$ scattering using the NCSM+RGM approach. The $A = 5$ system is an ideal testing ground for many-body scattering theory for several reasons: (i) the $A = 5$ system does not have a bound state; (ii) ^{4}He is tightly bound so that single-channel scattering is valid up to ~ 20 MeV; (iii) there are two low-lying p-wave resonances ($3/2^-$ and $1/2^-$); (iv) non-resonant s-wave scattering ($1/2^+$) for

	N_{max}	^{10}Be $E_{\mathrm{g.s.}}$	^{11}Be$(1/2^-)$ E	E_{th}	^{11}Be$(1/2^+)$ E	E_{th}
NCSM [180]	8/9	-57.06	-56.95	0.11	-54.26	2.80
NCSM [180]	6/7	-57.17	-57.51	-0.34	-54.39	2.78
NCSM+RGM [146]			-57.59	-0.42	-57.85	-0.68
Expt.		-64.98	-65.16	-0.18	-65.48	-0.50

Table 2. Energies (in MeV) of the ground state of ^{10}Be and the lowest states of ^{11}Be, calculated in NCSM using the CD-Bonn NN potential [74] at $\hbar\Omega = 13$ MeV. The NCSM+RGM results were obtained using $n+^{10}$Be configurations with $N_{\mathrm{max}} = 6$ g.s., 2_1^+, 2_2^+, and 1_1^+ states of ^{10}Be. (From Refs. [146, 180].)
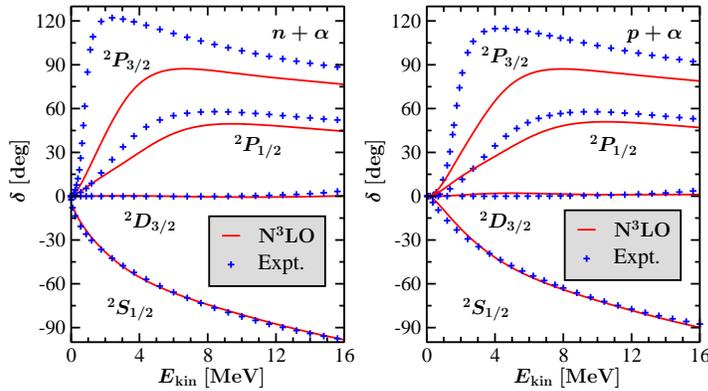
Figure 8. Calculated phase shifts for (left panel) n-α and (right panel) p-α scattering, using the N^{3}LO NN potential [81], compared to an R-matrix analysis of data (+). Theoretical results include the ^{4}He g.s., 0^+0, 0^-0, 1^-0, 1^-1, 2^-0, and 2^-1 states. (From Refs. [146, 162].)

which large effects of the Pauli exclusion principle is expected; (v) it is a well studied system. In particular, there have been recent microscopic studies of $N + \alpha$ scattering with GFMC [181] and NCSM+RGM [146, 147].

A comparison with an accurate R-matrix analysis of the nucleon-α scattering is presented in Fig. 8. It reveals that for both neutron (left panel) and proton (right panel) projectiles one can describe well the $^2S_{1/2}$ and, qualitatively, also the $^2D_{3/2}$ phase shifts, using the N^{3}LO NN potential. The good agreement of the N^{3}LO $^2S_{1/2}$ phase shifts with the R-matrix analysis can be credited to the repulsive action of the Pauli exclusion principle at short nucleon-α distances, which masks the short-range details of the nuclear interaction. On the other hand, the same interaction is not able to reproduce well the two P-wave phase shifts, which are both too small and too close to each other.

Recently, the NCSM+RGM approach was applied to a low-energy radiative capture reaction ^{7}Be$(p, \gamma)^8$B [149], and two fusion reactions ^{3}H$(d, n)^4$He and ^{3}He$(d, p)^4$He [150]. In all cases, a SRG evolved chiral EFT potential at two-body level was considered. It is important to realize that reaction calculations are extremely sensitive to the exact

positions of thresholds and resonances. In the studies mentioned above, the authors could utilize the model-dependence on the two-body SRG flow parameter to reproduce the experimental separation energies. This will, however, remain a particular challenge for *ab initio* reaction calculations starting from nuclear Hamiltonians which do not involve free parameters.

3.2. Neutron rich oxygen and calcium isotopes

The oxygen isotopic chain has been extensively studied experimentally during the last years, see for example Refs. [182, 183]. The neutron drip line has been tentatively established at ^{24}O, but the particle stability of ^{28}O is still a matter of a debate since the current experiments are on the limit of the production cross section. The isotopes ^{22}O ($N = 14$) and ^{24}O ($N = 16$) exhibit a doubly magic nature. Their structure is believed to be governed by the evolution of the $1s_{1/2}$ and $0d_{5/2}$ orbits. Recent experiments show that ^{25,26}O are unbound with respect to ^{24}O [184, 185]. On the other hand, the two-neutron drip line for the fluorine isotopes extends beyond ^{31}F. One speculates that the behavior of the neutron drip line for the oxygen and fluorine isotopic chains arise from a delicate balance between the proton-neutron and neutron-neutron interactions, the coupling to the continuum and 3NFs [45, 85, 87].

Another chain of isotopes crucial for theoretical developments is the calcium chain. It contains several possible closed-shell nuclei beyond the well established ones, namely ^{40}Ca and ^{48}Ca. The $N = 32$ sub-shell closure has been established from experiments on calcium [186, 187], titanium [188], and chromium [189]. The nucleus ^{52}Ca has a reduced value of 2_1^+ excitation (but more than twice as large as seen in open-shell calcium isotopes) than that observed in ^{48}Ca, suggesting a sub-shell closure. For ^{54}Ca ($N = 34$), no sub-shell closure has been seen experimentally in chromium [190] or titanium [191, 192], and there are some doubts regarding a sub-shell closure in calcium [193]. The heaviest calcium isotopes that have been observed are ^{57,58}Ca [194], but the masses have been measured only up to ^{52}Ca [195].

As emphasized in Sec. 2, to describe physics of nuclei near the drip lines, one needs to properly take into account (i) the effects of 3NFs, (ii) the presence of open decay channels and particle continuum, and (iii) many-nucleon correlations. Recently coupled-cluster calculations have been carried out for the binding energies and spectra of the neutron rich oxygen and calcium isotopes taking for the first time all these effects into account. The effects of 3NFs were included effectively in terms of density dependent corrections to the NN interaction. Those were derived from 3NFs by summing over the third particle in symmetric nuclear matter. This is obviously a departure from a rigorous *ab initio* approach, but nevertheless it is a first step towards including effects from both 3NFs and coupling to the particle continuum in coupled-cluster calculations. The continuum effects were included by using a Berggren basis for the relevant partial waves. The binding energies per particle for selected oxygen and calcium isotopes are displayed in Fig. 9. The inclusion of 3NFs significantly improves agreement with experiment. In
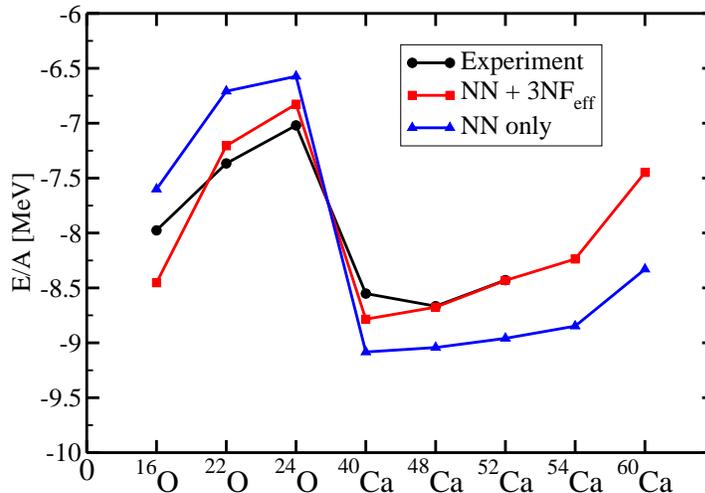
Figure 9. Binding energy per nucleon for selected oxygen and calcium isotopes calculated in coupled cluster theory with NN (triangles) and NN+3NF (red squares) forces, compared to experimental data (circles). (Based on Refs. [45, 87].)

order to investigate the evolution of shell structure and binding energy systematics in the neutron rich calcium isotopes in more detail, we show in Fig. 10 the total binding energies for very neutron rich calcium isotopes ranging from ^{48}Ca to ^{62}Ca. Several interesting features are apparent: (i) 3NFs are important; (ii) a peninsula of weak binding appears for the very neutron rich calcium isotopes ^{60,61,62}Ca, and (iii) the results with NN interactions only, do not yield a flattening of binding energy at large neutron numbers. Looking in more detail at the structure of $^{60-62}$Ca, we find the $J^\pi = 1/2^+_1$ ground state of ^{61}Ca slightly above the threshold, unbound by about 0.2 MeV with respect to ^{60}Ca, and entirely dominated by an s wave. Furthermore, the ordering of the gds shells is found to be reversed as compared to the standard shell model ordering. In particular, we find that the $5/2^+$ state appears below the $9/2^+$ state in ^{53,55,61}Ca. It is to be noted that the calculations employing the oscillator basis yield for ^{61}Ca the level ordering of the conventional shell model, with a $9/2^+$ ground state spin assignment, thus suggesting strong effects due to the continuum coupling. The nuclei ^{61}Ca and ^{62}Ca are predicted to be only weakly unbound with respect to ^{60}Ca.

Figure 11 shows the results for the 2^+_1 states in the neutron rich calcium isotopes. It is interesting to note that coupled-cluster calculations predict only a weak sub-shell closure in ^{54}Ca with a 2^+ state around 1.9 MeV. These examples clearly point tp the need for 3NFs in neutron-rich nuclei. Overall, we find that the effects of 3NFs and the scattering continuum are essential for understanding the evolution of shell structure towards the drip line. Although more investigations are clearly needed, our results hint at a situation where odd calcium isotopes beyond ^{60}Ca are unbound, while even isotopes can be weakly bound.

It is interesting to relate the coupled-cluster results for the Ca isotopes to those based on nuclear DFT. Figure 12 shows the two-neutron separation energies for even-
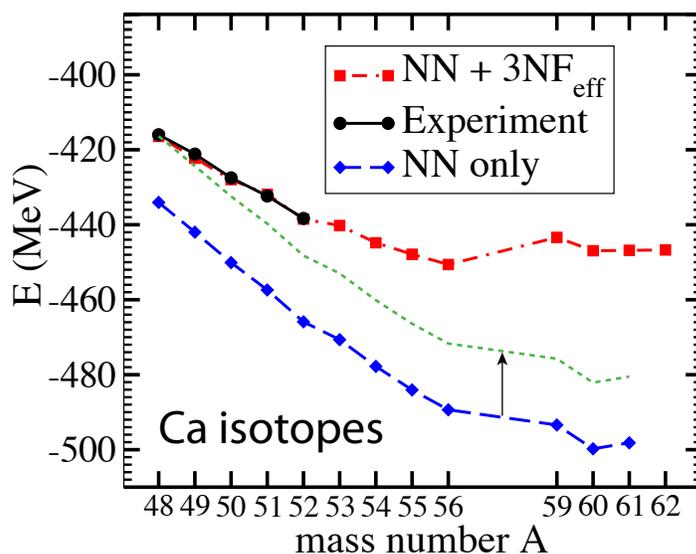
Figure 10. Binding energies of the neutron-rich calcium isotopes calculated in coupled cluster theory with NN (diamonds) and NN+3NF (squares) forces, compared to experimental data (circles). The dashed line indicates the NN result normalizes at ^{48}Ca. (Based on Ref. [87].)
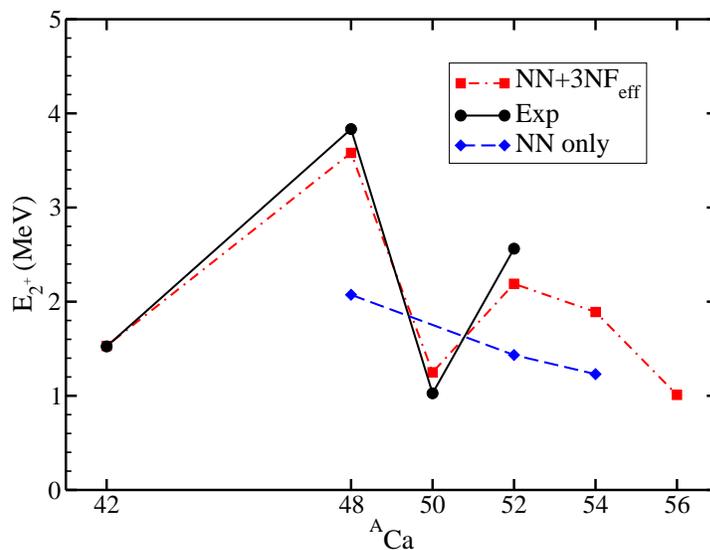

Figure 11. First 2^+ excited state energies for the calcium isotopes ^{42,48,50,52,54,56}Ca. Black circles: experimental data; blue diamonds: results from nucleon-nucleon interactions; red squares: results including the effects of three-nucleon forces. (Based on Ref. [87].)

even calcium isotopes computed in Ref. [8] using SLy4, SV-min, UNEDF0, and UNEDF1 EDFs and obtained in FRDM [196] and HFB-21 [197] mass models. All those models predict consistently the neutron drip line around ^{70}Ca. Interestingly, in all cases the two-neutron drip lins ($S_{2n} = 0$) is approached fairly gradually in all cases; this indicates that the neutron chemical potential $\lambda_n \approx -S_{2n}/2$ stays close to, but below, zero for $60 \leq N \leq 70$. A similar result was obtained in other DFT calculations [198–201]. As
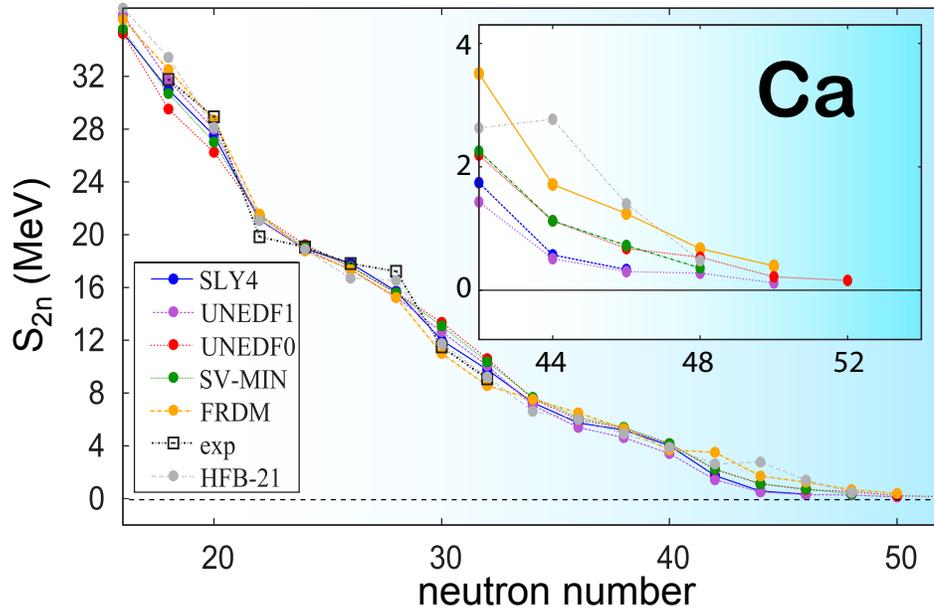
Figure 12. Theoretical extrapolations towards drip lines for the two-neutron separation energies S_{2n} for the isotopic chain of even-even calcium isotopes using different EDFs (SLy4, SV-min, UNEDF0, UNEDF1), and FRDM [196] and HFB-21 [197] mass models (see text for more details). All models are consistent with the available experimental data. Detailed predictions around $S_{2n} = 0$ are illustrated in the inset. Drawn by Erik Olsen based on Ref. [8].

discussed in Refs. [61, 202–205], the persistent appearance of λ_n just below the threshold can be associated with the continuum effect due to pairing. Indeed, the scattering of neutron pairs into the close-lying non-resonant continuum gives rise to a stabilization of binding energy and a very weak dependence of λ_n on N; hence, extension of the range of bound nuclei. In terms of HFB quasiparticles, this continuum coupling manifests itself through increased occupations of low-lying quasi-particle states, especially those having low orbital angular momentum [202], as one approaches the threshold. This results in a gradual increase of contribution from nonresonant continuum to the ground state of the system.

By looking at canonical HFB states, one can notice the emergence of bound canonical orbits from the single-neutron continuum. For the considered case of the drip line Ca nuclei, the canonical neutron states $s_{1/2}$, $d_{5/2}$, and $d_{3/2}$ appear very close to the bound $g_{9/2}$ level, which is expected to form the valence shell in the traditional shell model [198]. The fact that high-ℓ and low-ℓ orbits bunch up very close to the $\lambda_n = 0$

threshold creates an opportunity for other correlations to further lower the binding energy. Figure 13 shows the isoscalar (mass) ground-state quadrupole deformations
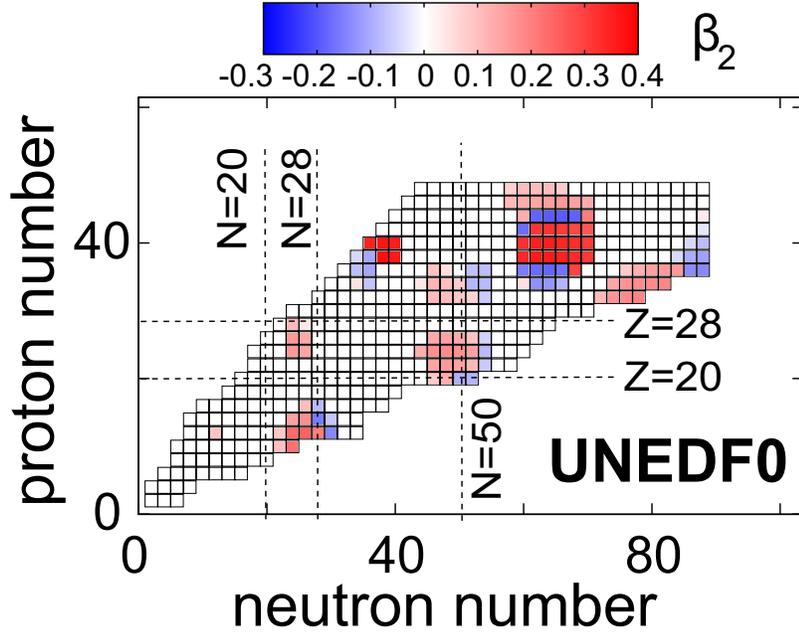

Figure 13. Isoscalar quadrupole deformation β_2 for $Z < 50$ even-even nuclei predicted in HFB calculations with UNEDF0 energy density functional [67]. The neutron-rich Ca isotopes with $N \approx 50$ are predicted to be deformed. (Based on Ref. [8].)

in $Z < 50$ even-even nuclei calculated in the HFB+UNEDF0 model in Ref. [8]. The appearance of deformation around ^{70}Ca is clearly seen. For more discussion on deformed drip line nuclei, see Refs. [8, 205–208].

The binding energy stabilization close to the threshold appears naturally in the continuum shell model through the collective coupling of shell model states via the decay channel [209, 210]. This coupling, governed by the anti-Hermitian term in the effective Hamiltonian that represents the continuum coupling, leads to the formation of the collective aligned state. The mechanism responsible for the creation of an aligned state is similar to the formation mechanism of super-radiant states [211, 212]. In this language, the behavior of drip line Ca isotopes, the particle stability of ^{6,8}He and ^{11}Li, and the appearance of cluster states near the reaction threshold that exhausts most of the decay width, are all manifestations of the same emergent near-threshold phenomenon [209, 210].

Clearly, it would be very interesting to see if *ab initio* approaches confirm the trends predicted in nuclear DFT. The fact that the coupled-cluster calculations of Ref. [87] yield a $J^\pi = 1/2^+$ ground state for ^{61}Ca, unlike the shell ordering in the conventional shell model, is a tantalizing hint that this is indeed the case.

4. Conclusions and perspectives

In this contribution, we have demonstrated that modern many-body techniques are nowadays capable of providing a reliable description of nuclear properties thanks to new conceptual insights as well as algorithmic and computational advances. For light nuclei, like the chain of lithium and beryllium isotopes, no-core shell-model calculations provide an invaluable tool to link nuclear structure to the underlying forces. Similarly, coupled cluster theory that includes 3NFs and coupling to the particle continuum, is capable of providing reliable predictions for heavier nuclei such as oxygen and calcium isotopes. Modern nuclear density functional theory, with optimized energy density functionals, provides an excellent description of heavy nuclei, and it links to *ab initio* approaches as well. Recent parametrizations of nuclear energy density functionals provide fairly consistent predictions when extrapolated to mass regions where experimental data are not available. Close to the limits of stability, the degrees of freedom represented by resonances, weakly bound states and the non-resonant continuum need to be accounted for properly. The latter has important consequences for the interpretation of rare isotopes in terms of a naive shell-model picture. Our results indicate that this traditional picture may not be relevant close to the neutron drip line. All of this holds great promise for a quantitative and predictive modeling of nuclei from a bottom-up perspective.

It is important to emphasize that the nuclear many-body problem is a splendid example of a multiscale problem, with length scales spanning many decades. A description of multiscale processes entails different theoretical methods for different length scales. First-principle methods are limited to few interacting nucleons. With an increasing number of degrees of freedom, DFT-based methods become the methods of choice. For even larger systems, a molecular-dynamics-based modeling is the favored approach. To link these different scales and methods properly is a great challenge not only to nuclear physics, but to fields as diverse as material science and life science, see for example Ref. [213].

In this work, we have illustrated some challenges and opportunities of the modern nuclear many-body problem, especially in the context of rare isotopes. In particular, we have emphasized the need for a high quality input, the importance of many-body dynamics and the impact of the coupling to open channels, summarized in Fig. 14. With a fundamental picture of nuclei based on the correct microphysics, we can remove the empiricism inherent today, giving us thereby a greater confidence in the science we deliver and the predictions we make. Guided by unique data on rare isotopes, we are embarking on a comprehensive study of *all nuclei*, based on the most accurate knowledge of nuclear interactions, the most reliable theoretical approaches, and massive use of new computer hardware and advanced numerical algorithms. The prospects are excellent.
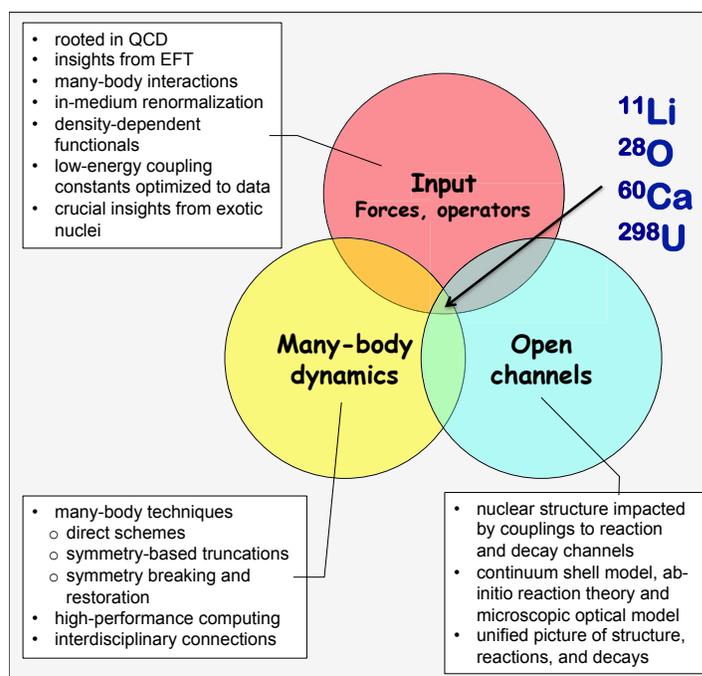
Figure 14. Challenges of the nuclear many-body problem. A comprehensive theoretical framework that would be quantitative, have predictive power, and provide uncertainty quantification must meet three stringent requirements: (i) the input must be quantified and of high quality; (ii) many-body dynamics and correlations must be accounted for; and (iii) the associated formalism must take care of open-quantum-system aspects of the nucleus. Only then can we hope to understand rare isotopes, such as ^{11}Li (two-neutron halo), ^{28}O (doubly-magic, probably unbound), ^{60}Ca (territory for new physics, where *ab initio* theory and DFT meet), and ^{298}U (r-process system, fission recycling participant),

[1] 2007 *Scientific Opportunities with a Rare-Isotope Facility in the United States*. The National Academies Press
[2] 2012 *Nuclear Physics: Exploring the Heart of Matter*. The National Academies Press
[3] Dobaczewski J and Nazarewicz W 1998 *Phil. Trans. R. Soc. Lond. A* **356** 2007
[4] Thoennessen M and Sherrill B 2011 *Nature* **473** 25
[5] Brown B 2001 *Prog. Part. Nucl. Phys.* **47** 517
[6] Baumann T, Spyrou A and Thoennessen M 2012 *Rep. Prog. Phys.* **75** 036301
[7] Sorlin O and Porquet M G 2008 *Prog. Part. Nucl. Phys.* **61** 602
[8] Erler J, Birge N, Kortelainen M, Nazarewicz W, Olsen E, Perhac A M and Stoitsov M 2012 *Nature* **486** 509
[9] Epelbaum E, Hammer H W and Meißner U G 2009 *Rev. Mod. Phys.* **81** 1773
[10] Machleidt R and Entem D 2011 *Phys. Rep.* **503** 1
[11] Kvaal S 2009 *Phys. Rev. B* **80** 045321
[12] Furnstahl R J, Hagen G and Papenbrock T 2012 *Phys. Rev. C* **86** 031301
[13] Hjorth-Jensen M, Dean D, Hagen G and Kvaal S 2010 *J. Phys. G: Nucl. Part. Phys.* **37** 064035
[14] Coon S A, Avetian M I, Kruse M K G, van Kolck U, Maris P and Vary J P 2012 *Phys. Rev. C* **86** 054002
[15] Bertsch G F, Dean D J and Nazarewicz W 2007 *SciDAC Review* **6** 42
[16] Furnstahl R J 2011 *Nucl. Phys. News* **21** 18
[17] Schatz H et al. 1998 *Phys. Rep.* **294** 167
[18] Langanke K and Wiescher M 2001 *Rep. Prog. Phys.* **64** 1657
[19] Sherill B 2012 private communication
[20] Michel N, Nazarewicz W, Płoszajczak M and Vertse T 2009 *J. Phys. G* **36** 013101
[21] Dobaczewski J, Michel N, Nazarewicz W, Płoszajczak M and Rotureau J 2007 *Prog. Part. Nucl. Phys.* **59** 432
[22] Shavitt I and Bartlett R J 2009 *Many-body Methods in Chemistry and Physics* (Cambridge University Press)
[23] Helgaker T, Jørgensen P and Olsen J 2000 *Molecular Electronic Structure Theory. Energy and Wave Functions* (Chichester: Wiley)
[24] Hagen G, Papenbrock T, Dean D J and Hjorth-Jensen M 2010 *Phys. Rev. C* **82** 034330
[25] Pieper S C and Wiringa R B 2001 *Annual Review of Nuclear and Particle Science* **51** 53
[26] Koonin S, Dean D and Langanke K 1997 *Phys. Rep.* **278** 1
[27] Utsuno Y, Otsuka T, Mizusaki T and Honma M 1999 *Phys. Rev. C* **60** 054315
[28] Hjorth-Jensen M, Kuo T T and Osnes E 1995 *Phys. Rep.* **261** 125
[29] Dickhoff W H and Neck D V 2005 *Many-Body Theory exposed!* (World Scientific)
[30] Barbieri C and Dickhoff W H 2004 *Prog. Part. Nucl. Phys.* **52** 377
[31] Roth R, Hergert H, Papakonstantinou P, Neff T and Feldmeier H 2005 *Phys. Rev. C* **72** 034002
[32] White S R 1992 *Phys. Rev. Lett.* **69** 2863
[33] Schollwock U 2005 *Rev. Mod. Phys.* **77** 259
[34] Rotureau J, Michel N, Nazarewicz W, Płoszajczak M and Dukelsky J 2009 *Phys. Rev. C* **79** 014304
[35] Bartlett R J, Lotrich V F and Schweigert I V 2005 *J. Chem. Phys.* **123** 062205
[36] Tsukiyama K, Bogner S K and Schwenk A 2011 *Phys. Rev. Lett.* **106** 222502
[37] Hergert H, Bogner S K, Binder S, Calci A, Langhammer J, Roth R and Schwenk A 2012 *arXiv:1212.1190[nucl-th]*
[38] Caurier E, Martinez-Pinedo G, Nowacki F, Poves A and Zuker A P 2005 *Rev. Mod. Phys.* **77** 427

[39] Navrátil P, Quaglioni S, Stetcu I and Barrett B R 2009 *J. Phys. G* **36** 083101
[40] Pudliner B S, Pandharipande V R, Carlson J, Pieper S C and Wiringa R B 1997 *Phys. Rev. C* **56** 1720
[41] Pieper S C, Pandharipande V R, Wiringa R B and Carlson J 2001 *Phys. Rev. C* **64** 014001
[42] Wiringa R B and Pieper S C 2002 *Phys. Rev. Lett.* **89** 182501
[43] Navrátil P and Barrett B R 1998 *Phys. Rev. C* **57** 562
[44] Navrátil P, Vary J P and Barrett B R 2000 *Phys. Rev. Lett.* **84** 5728
[45] Hagen G, Hjorth-Jensen M, Jansen G R, Machleidt R and Papenbrock T 2012 *Phys. Rev. Lett.* **108** 242501
[46] Roth R, Binder S, Vobig K, Calci A, Langhammer J and Navrátil P 2012 *Phys. Rev. Lett.* **109** 052501
[47] Binder S, Langhammer J, Calci A, Navratil P and Roth R 2012 *arXiv:1211.4748[nucl-th]*
[48] Michel N, Nazarewicz W, Płoszajczak M and Vertse T 2009 *J. Phys. G* **36** 013101
[49] Berggren T 1968 *Nucl. Phys. A* **109** 265
[50] Berggren T and Lind P 1993 *Phys. Rev. C* **47** 768
[51] Lind P 1993 *Phys. Rev. C* **47** 1903
[52] Hagen G, Hjorth-Jensen M and Michel N 2006 *Phys. Rev. C* **73** 064307
[53] Hagen G, Dean D J, Hjorth-Jensen M and Papenbrock T 2007 *Phys. Lett. B* **656** 169
[54] Papadimitriou G et al. 2012 private communication
[55] Bender M, Heenen P H and Reinhard P G 2003 *Rev. Mod. Phys.* **75** 121
[56] Gandolfi S, Carlson J and Pieper S C 2011 *Phys. Rev. Lett.* **106** 012501
[57] Bogner S K, Furnstahl R J, Hergert H, Kortelainen M, Maris P, Stoitsov M and Vary J P 2011 *Phys. Rev. C* **84** 044306
[58] Kortelainen M, McDonnell J, Nazarewicz W, Reinhard P G, Sarich J, Schunck N, Stoitsov M V and Wild S M 2012 *Phys. Rev. C* **85** 024304
[59] J. Dobaczewski H. Flocard J T 1984 *Nucl. Phys. A* **422** 103
[60] Dobaczewski J, Nazarewicz W, Werner T, Berger J, Chinn C and Decharge J 1996 *Phys. Rev. C* **53** 2809
[61] Dobaczewski J and Nazarewicz W 2012 *50 Years of Nuclear BCS, edited by R. A. Broglia and V. Zelevinsky* (World Scientific)
[62] Pei J C, Kruppa A T and Nazarewicz W 2011 *Phys. Rev. C* **84** 024311
[63] Stoitsov M, Michel N and Matsuyanagi K 2008 *Phys. Rev. C* **77** 054301
[64] Michel N, Matsuyanagi K and Stoitsov M 2008 *Phys. Rev. C* **78** 044319
[65] Klüpfel P, Reinhard P G, Bürvenich T J and Maruhn J A 2009 *Phys. Rev. C* **79** 034310
[66] Reinhard P G and Nazarewicz W 2010 *Phys. Rev. C* **81** 051303
[67] Kortelainen M 2010 *Phys. Rev. C* **82** 024313
[68] Fattoyev F J and Piekarewicz J 2011 *Phys. Rev. C* **84** 064302
[69] Beane S R, Bedaque P F, Orginos K and Savage M J 2006 *Phys. Rev. Lett.* **97** 012001
[70] Ishii N, Aoki S and Hatsuda T 2007 *Phys. Rev. Lett.* **99** 022001
[71] Aoki S, Hatsuda T and Ishii N 2010 *Progress of Theoretical Physics* **123** 89
[72] Beane S R et al. 2012 *Phys. Rev. D* **85** 054511
[73] S.R. Beane et al. 2012 *arXiv:1206.5219[hep-lat]*
[74] Machleidt R 2001 *Phys. Rev. C* **63** 024001
[75] Wiringa R B, Stoks V G J and Schiavilla R 1995 *Phys. Rev. C* **51** 38
[76] Stoks V, Klomp R, Terheggen C and de Swart J 1994 *Phys. Rev. C* **49** 2950
[77] Engvik L, Hjorth-Jensen M, Machleidt R, Müther H and Polls A 1997 *Nucl. Phys. A* **627** 85
[78] Weinberg S 1990 *Phys. Lett. B* **363** 288
[79] Kolck U V 1999 *Prog. Part. Nucl. Phys.* **43** 337
[80] Epelbaum E, Krebs H, Lee D and Meißner U G 2011 *Phys. Rev. Lett.* **106** 192501
[81] Entem D R and Machleidt R 2003 *Phys. Rev. C* **68** 041001
[82] Kalantar-Nayestanaki N, Epelbaum E, Messchendorp J G and Nogga A 2012 *Rep. Prog. Phys.*

75 016301

[83] Hebeler K, Bogner S K, Furnstahl R J, Nogga A and Schwenk A 2011 *Phys. Rev. C* **83** 031301

[84] Maris P, Vary J P, Navrátil P, Ormand W E, Nam H and Dean D J 2011 *Phys. Rev. Lett.* **106** 202502

[85] Otsuka T, Suzuki T, Holt J D, Schwenk A and Akaishi Y 2010 *Phys. Rev. Lett.* **105** 032501

[86] Holt J D, Otsuka T, Schwenk A and Suzuki T 2012 *J. Phys. G* **39** 085111

[87] Hagen G, Hjorth-Jensen M, Jansen G R, Machleidt R and Papenbrock T 2012 *Phys. Rev. Lett.* **109** 032502

[88] Hebeler K, Lattimer J M, Pethick C J and Schwenk A 2010 *Phys. Rev. Lett.* **105** 161102

[89] Gandolfi S, Carlson J and Reddy S 2012 *Phys. Rev. C* **85** 032801

[90] Steiner A W and Gandolfi S 2012 *Phys. Rev. Lett.* **108** 081102

[91] Suzuki K and Lee S Y 1980 *Prog. Theor. Phys.* **64** 2091

[92] Suzuki K 1982 *Progr.Theor.Phys.* **68** 246

[93] Suzuki K and Okamoto R 1994 *Prog. Theor. Phys.* **92** 1045

[94] Suzuki K and Okamoto R 1995 *Progr.Theor.Phys.* **93** 905

[95] Kvaal S 2008 *Phys. Rev. C* **78** 044330

[96] Navrátil P, Kamuntavičius G P and Barrett B R 2000 *Phys. Rev. C* **61** 044001

[97] Bogner S, Furnstahl R and Schwenk A 2010 *Prog. Part. Nucl. Phys.* **65** 94

[98] Epelbaoum E, Glöckle W, Krüger A and Meißner U G 1999 *Nucl. Phys. A* **645** 413

[99] Bogner S K, Kuo T T S and Schwenk A 2003 *Phys. Rep.* **386** 1

[100] Bogner S K, Schwenk A, Furnstahl R J and Nogga A 2005 *Nucl. Phys. A* **763** 59

[101] Głazek S D and Wilson K G 1993 *Phys. Rev. D* **48** 5863

[102] Wegner F 1994 *Annalen der Physik* **506** 77

[103] Bogner S K, Furnstahl R J and Perry R J 2007 *Phys. Rev. C* **75** 061001

[104] Jurgenson E D, Navrátil P and Furnstahl R J 2009 *Phys. Rev. Lett.* **103** 082501

[105] Roth R, Langhammer J, Calci A, Binder S and Navrátil P 2011 *Phys. Rev. Lett.* **107** 072501

[106] Åkerlund O, Lindgren E J, Bergsten J, Grevholm B, Lerner P, Linscott R, Forssén C and Platter L 2011 *European Physical Journal A* **47** 122

[107] Hebeler K 2012 *Phys. Rev. C* **85** 021002

[108] Dean D, Engeland T, Hjorth-Jensen M, Kartamyshev M and Osnes E 2004 *Prog. Part. Nucl. Phys.* **53** 419

[109] Horoi M, Gour J R, Włoch M, Lodriguito M D, Brown B A and Piecuch P 2007 *Phys. Rev. Lett.* **98** 112501

[110] Mizusaki T, Honma M and Otsuka T 1996 *Phys. Rev. C* **53** 2786

[111] Honma M, Mizusaki T and Otsuka T 1996 *Phys. Rev. Letters* **77** 3315

[112] Booth G H and Alavi A 2010 *The J. Chem. Phys.* **132** 174104

[113] Coester F 1958 *Nuclear Physics* **7** 421

[114] Kümmel H, Lührmann K H and Zabolitzky J G 1978 *Phys. Rep.* **36** 1

[115] Heisenberg J H and Mihaila B 1999 *Phys. Rev. C* **59** 1440

[116] Dean D J and Hjorth-Jensen M 2004 *Phys. Rev. C* **69** 054320

[117] Bartlett R J and Musiał M 2007 *Rev. Mod. Phys.* **79** 291

[118] Golub G and Van Loan C 1996 *Matrix Computations* (John Hopkins University Press)

[119] Kucharski S A and Bartlett R J 1998 *The J. Chem. Phys.* **108** 5243

[120] Taube A G and Bartlett R J 2008 *The J. Chem. Phys.* **128** 044110

[121] Hagen G, Papenbrock T, Dean D J and Hjorth-Jensen M 2008 *Phys. Rev. Lett.* **101** 092502

[122] Jansen G R, Hjorth-Jensen M, Hagen G and Papenbrock T 2011 *Phys. Rev. C* **83** 054306

[123] Michel N, Nazarewicz W, Okołowicz J and Płoszajczak M 2010 *J. Phys. G* **37** 064042

[124] Bennaceur K, Nowacki F, Okołowicz J and Płoszajczak M 1999 *Nucl. Phys. A* **651** 289

[125] Okołowicz J, Płoszajczak M and Rotter I 2003 *Phys. Rep.* **374** 271

[126] Volya A and Zelevinsky V 2005 *Phys. Rev. Lett.* **94** 052501

[127] Rotureau J, Okołowicz J and Płoszajczak M 2005 *Phys. Rev. Lett.* **95** 42503

[128] Feshbach H 1964 *Rev. Mod. Phys.* **36** 1076
[129] Michel N, Nazarewicz W, Płoszajczak M and Bennaceur K 2002 *Phys. Rev. Lett.* **89** 042502
[130] Michel N, Nazarewicz W, Płoszajczak M and Okołowicz J 2003 *Phys. Rev. C* **67** 54311
[131] IdBetan R, Liotta R J, Sandulescu N and Vertse T 2003 *Phys. Rev. C* **67** 14322
[132] Michel N, Nazarewicz W and Płoszajczak M 2007 *Phys. Rev. C* **75** 0311301(R)
[133] Michel N, Nazarewicz W and Płoszajczak M 2007 *Nucl. Phys. A* **794** 29
[134] Michel N, Nazarewicz W and Płoszajczak M 2010 *Phys. Rev. C* **82** 044315
[135] Papadimitriou G, Kruppa A T, Michel N, Nazarewicz W, Płoszajczak M and Rotureau J 2011 *Phys. Rev. C* **84** 051304(R)
[136] Okołowicz J, Michel N, Nazarewicz W and Płoszajczak M 2012 *Phys. Rev. C* **85** 064320
[137] White S R 1993 *Phys. Rev. B* **48** 10345
[138] Roman J M, Sierra G and Dukelsky J 2002 *Nucl. Phys. B* **634** 483
[139] Pittel S and Sandulescu N 2006 *Phys. Rev. C* **73** 014301
[140] Papenbrock T and Dean D J 2005 *J. Phys. G* **31** 1377
[141] Thakur B, Pittel S and Sandulescu N 2008 *Phys. Rev. C* **78** 041303
[142] Rotureau J, Michel N, Nazarewicz W, Płoszajczak M and Dukelsky J 2006 *Phys. Rev. Lett.* **97** 110603
[143] Carlon E, Henkel M and Schollwöck U 1999 *European Physical Journal B* **12** 99
[144] McCulloch I P and Gulácsi M 2002 *EPL (Europhysics Letters)* **57** 852
[145] Wildermuth K and Tang Y C 1977 *A unified theory of the nucleus* (Vieweg, Braunschweig [Ger.])
[146] Quaglioni S and Navrátil P 2008 *Phys. Rev. Lett.* **101** 092501
[147] Quaglioni S and Navrátil P 2009 *Phys. Rev. C* **79** 044606
[148] Navrátil P, Roth R and Quaglioni S 2010 *Phys. Rev. C* **82** 034609
[149] Navrátil P and Quaglioni S 2011 *Phys. Rev. C* **83** 044609
[150] Navrátil P and Quaglioni S 2012 *Phys. Rev. Lett.* **108** 042503
[151] Otsuka T, Fujimoto R, Utsuno Y, Brown B A, Honma M and Mizusaki T 2001 *Phys. Rev. Lett.* **87** 082502
[152] Otsuka T, Suzuki T, Fujimoto R, Grawe H and Akaishi Y 2005 *Phys. Rev. Lett.* **95** 232502
[153] Honma M, Otsuka T, Brown B A and Mizusaki T 2002 *Phys. Rev. C* **65** 061301
[154] Leidemann W and Orlandini G 2012 *Prog. Part. Nucl. Phys.*
[155] Barnea N, Leidemann W and Orlandini G 2000 *Phys. Rev. C* **61** 054001
[156] Barnea N, Leidemann W and Orlandini G 2001 *Nucl. Phys. A* **693** 565
[157] Epelbaum E, Krebs H, Lee D and Meißner U G 2010 *Phys. Rev. Lett.* **104** 142501
[158] Hagen G, Papenbrock T, Dean D J, Schwenk A, Nogga A, Wloch M and Piecuch P 2007 *Phys. Rev. C* **76** 034302
[159] Navrátil P, Vary J P and Barrett B R 2000 *Phys. Rev. C* **62** 054311
[160] Navrátil P, Gueorguiev V G, Vary J P, Ormand W E and Nogga A 2007 *Phys. Rev. Lett.* **99** 042501
[161] Kievsky A, Rosati S, Viviani M, Marcucci L E and Girlanda L 2008 *J. Phys. G* **35** 063101
[162] Forssén C, Navrátil P and Quaglioni S 2011 *Few-Body Systems* **49** 11
[163] Roth R and Navrátil P 2007 *Phys. Rev. Lett.* **99** 092501
[164] Mueller P et al. 2007 *Phys. Rev. Lett.* **99** 252501
[165] Brodeur M et al. 2012 *Phys. Rev. Lett.* **108** 052504
[166] Pieper S C 2008 *Nuovo Cimento Rivista Serie* **31** 709
[167] Caurier E and Navrátil P 2006 *Phys. Rev. C* **73** 021302
[168] Neff T, Feldmeier H and Roth R 2005 *Nucl. Phys. A* **752** 321
[169] Bacca S, Schwenk A, Hagen G and Papenbrock T 2009 *European Physical Journal A* **42** 553
[170] Hagen G, Dean D J, Hjorth-Jensen M and Papenbrock T 2007 *Phys. Lett. B* **656** 169
[171] Alkhazov G D et al. 1997 *Phys. Rev. Lett.* **78** 2313
[172] Simon H et al. 2007 *Nucl. Phys. A* **791** 267
[173] Forssén C, Caurier E and Navrátil P 2009 *Phys. Rev. C* **79** 021303

[174] Doleschall P 2004 *Phys. Rev. C* **69** 054001

[175] Forssén C, Vary J P, Caurier E and Navrátil P 2008 *Phys. Rev. C* **77** 024301

[176] Furnstahl R J, Hagen G and Papenbrock T 2012 *Phys. Rev. C* **86** 031301

[177] Marcucci L E, Pervin M, Pieper S C, Schiavilla R and Wiringa R B 2008 *Phys. Rev. C* **78** 065501

[178] Unkelbach M and Hofmann H M 1991 *Few-Body Systems* **11** 143

[179] Neugart R et al. 2008 *Phys. Rev. Lett.* **101** 132502

[180] Forssén C, Navrátil P, Ormand W E and Caurier E 2005 *Phys. Rev. C* **71** 044312

[181] Nollett K M, Pieper S C, Wiringa R B, Carlson J and Hale G M 2007 *Phys. Rev. Lett.* **99** 022502

[182] Hoffman C R et al. 2009 *Phys. Lett. B* **672** 17

[183] Kanungo R et al. 2009 *Phys. Rev. Lett.* **102** 152501

[184] Hoffman C R et al. 2008 *Phys. Rev. Lett.* **100** 152502

[185] Lunderberg E et al. 2012 *Phys. Rev. Lett.* **108** 142503

[186] Huck A, Klotz G, Knipper A, Miehé C, Richard-Serre C, Walter G, Poves A, Ravn H L and Marguier G 1985 *Phys. Rev. C* **31** 2226

[187] Gade A et al. 2006 *Phys. Rev. C* **74** 021302

[188] Janssens R et al. 2002 *Phys. Lett. B* **546** 55

[189] Prisciandaro J et al. 2001 *Phys. Lett. B* **510** 17

[190] Marginean N et al. 2006 *Phys. Lett. B* **633** 696

[191] Liddick S N et al. 2004 *Phys. Rev. Lett.* **92** 072502

[192] Dinca D C et al. 2005 *Phys. Rev. C* **71** 041302

[193] Rejmund M et al. 2007 *Phys. Rev. C* **76** 021304

[194] Tarasov O B et al. 2009 *Phys. Rev. C* **80** 034609

[195] Gallant A T et al. 2012 *Phys. Rev. Lett.* **109** 032506

[196] Möller P, Nix J R and Myres Swiatecki W J 1995 *At. Data and Nuc. Data Tables* **59** 185

[197] Goriely S, Chamel N and Pearson J M 2010 *Phys. Rev. C* **82** 035804

[198] Meng J, Toki H, Zeng J Y, Zhang S Q and Zhou S G 2002 *Phys. Rev. C* **65** 041302

[199] Bhattacharya M and Gangopadhyay G 2005 *Phys. Rev. C* **72** 044318

[200] Sandulescu N, Geng L S, Toki H and Hillhouse G C 2003 *Phys. Rev. C* **68** 054323

[201] Grasso M, Yoshida S, Sandulescu N and Van Giai N 2006 *Phys. Rev. C* **74** 064317

[202] Fayans S A, Tolokonnikov S V and Zawischa D 2000 *Phys. Lett. B* **491** 245

[203] Rotival V, Bennaceur K and Duguet T 2009 *Phys. Rev. C* **79** 054309

[204] Zhang Y, Matsuo M and Meng J 2011 *Phys. Rev. C* **83** 054301

[205] Li L, Meng J, Ring P, Zhao E G and Zhou S G 2012 *Phys. Rev. C* **85** 024312

[206] Misu T, Nazarewicz W and Åberg S 1997 *Nucl. Phys. A* **614** 44

[207] Stoitsov M V 2003 *Phys. Rev. C* **68** 054312

[208] Chen Y, Li L, Liang H and Meng J 2012 *Phys. Rev. C* **85** 067301

[209] Okołowicz J, Płoszajczak M and Nazarewicz W 2012 *Prog. Theor. Phys. Supplement* **196** 230

[210] Okołowicz J, Nazarewicz W and Płoszajczak M 2012 *Fortschritte der Physik, Special Issue related to Quantum Physics with Non-Hermitian Operators; arXiv:1207.6225*

[211] Sokolov V and Zelevinsky V 1989 *Nucl. Phys. A* **504** 562

[212] Drożdż S, Okołowicz J, Płoszajczak M and Rotter I 2000 *Phys. Rev. C* **62** 024313

[213] Kirchner B and Vrabec J E 2012 *Multiscale Molecular Methods in Applied Chemistry* vol. 307 (Berlin, Germany: Springer)